Report No. 515

IMPROVED QUANTIFICATION OF STORMWATER DILUTION IN WASTEWATER TREATMENT PLANT INFLUENT USING ORGANIC MATER FLUORESCENCE

By
Christopher L. Osburn and Sara Gabriela Cornejo Zepeda

Department of Marine, Earth, and Atmospheric Sciences
NC State University
Raleigh, NC

wrri.ncsu.edu
NC WATER RESOURCES RESEARCH INSTITUTE

UNC-WRRI-515

The research on which this report is based was supported by funds provided by the North Carolina General Assembly and/or the US Geological Survey through the North Carolina Water Resources Research Institute.

WRRI Project No. 24-07-W
November 20, 2025

wrri.ncsu.edu
NC WATER RESOURCES RESEARCH INSTITUTE

Improved Quantification of Stormwater Dilution in Wastewater Treatment Plant Influent using Organic Matter Fluorescence

FINAL REPORT

Christopher L. Osburn* and Sara Gabriela Cornejo Zepeda

Department of Marine, Earth, and Atmospheric Sciences

North Carolina State University

Raleigh, North Carolina

27695

WRRI-USGS 104b Project Number 23-10-W

*Email: closburn@ncsu.edu; Tel: +1.919.515.0382

Abstract

Improved Quantification of Stormwater Dilution in Wastewater Treatment Plant Influent using Organic Matter Fluorescence. Wastewater treatment plants (WWTPs) are designed to process residential and industrial sewer flow as influent; however, they often receive additional water during and after rainfall through inflow and infiltration (I&I). These unplanned inputs dilute the influent, reduce treatment efficiency, and increase operational costs. The objective of this study was to use organic matter fluorescence in a source apportionment model (FluorMod) to detect and quantify I&I contributions to WWTP influent. A reference library of 142 excitation-emission matrices (EEMs) was developed, representing six potential sources: wastewater, rainwater, groundwater, river water, soil leachate, and street runoff. Samples from ten municipal WWTPs across North Carolina were analyzed, including facilities spanning both the Coastal Plain and Piedmont regions. Each sources' contributions to each unknown sample were estimated using FluorMod and, coupled with descriptive statistics, Pearson correlation, and time-series analysis, we gained insight into the variability and dynamics of I&I.

Two Coastal Plain WWTPs showed median influent dilution by groundwater exceeding 83%, while others showed variable contributions from both rainwater and groundwater, with an overall median dilution of 16% and 9% respectively. Several Piedmont WWTPs showed median dilution values near 0%, only exhibiting episodic dilution events following substantial five-day antecedent precipitation (AP_5). In several systems, the number of contributing I&I sources increased with higher AP_5, consistent with rainfall activating additional inflow and infiltration pathways. Higher and chronic groundwater dilution occurred in the Coastal Plain relative to the Piedmont. However, the observed variability in I&I dynamics suggests that other factors including, but not limited to, sewer infrastructure condition, hydraulic connectivity, soil saturation, geologic setting, and the spatial distribution of rainfall, likely play significant roles in modulating dilution behavior.

Results for each plant were disseminated in two outreach efforts. First, reports that summarized the project scope, methods, and time series results were shared with each plant shared. Second, offers for an online discussion of results and deeper explanation of the FluorMod approach were made, culminating in three Zoom meetings held prior to the end of the project.

Project results demonstrate that fluorescence-based source apportionment is a practical, cost-effective tool for identifying and quantifying I&I contributions from multiple sources. Future applications extend to exfiltration of sewage and other potential pollution sources that carry a fluorescence signature. The project outcomes represent a substantial innovative method to corroborate results from other I&I methods and investigate I&I issues in sewersheds at scale. FluorMod's adaptability and accessibility make it a promising diagnostic for WWTP operators and may complement conventional field techniques to support more targeted infrastructure assessments, long-term monitoring, and investment planning to address I&I challenges.

1. Introduction

Wastewater treatment plants (WWTPs) receive domestic and industrial sewage. WWTPs use physical, chemical, and biological processes to reduce organic matter, nutrients, and pathogens in the influent to meet regulatory discharge standards (Carey & Migliaccio, 2009). This treatment is essential for protecting downstream water quality, aquatic ecosystems, and public health (Englande et al., 2015).

Wastewater infrastructure also includes extensive sewer collection systems — networks of pipelines converging into interceptors that deliver wastewater to treatment plants (Hanke & Wentworth, 1981). Gravity moves wastewater from the sewershed, though pump stations are needed in low-lying areas. Manholes, placed for inspection and maintenance, also create entry points for unwanted flow.

Historically, cities built combined sewer systems, transporting sanitary wastewater and stormwater in the same pipes. These systems often included combined sewer overflow (CSO) structures to discharge excess flow during rain events. While this prevented urban flooding, it released untreated sewage into receiving waters, risking public health and ecosystems (US Environmental Protection Agency, 2004). Consequently, most municipalities transitioned to separate sanitary sewer systems, carrying only wastewater, with stormwater managed separately.

However, even separate systems are vulnerable to external inputs from installation flaws or aging infrastructure. Pipes develop cracks from ground settlement, tree root intrusion, or poor joints. Older materials (e.g., terra cotta clay) are particularly susceptible. This damage allows external water (stormwater, groundwater, snowmelt) to enter, causing flows to deviate from the intended sanitary wastewater.

These vulnerabilities are inflow and infiltration (I&I): the unintended entry of stormwater and groundwater into sewer networks, a persistent challenge for separate systems. Excessive I&I can exceed capacity, leading to sanitary sewer overflows (SSOs), sewer backups, or bypass flows at WWTPs. Inflow is stormwater entry through improper connections (e.g., roof downspouts) (Environmental Protection Agency, 2004) and is typically episodic, tied to precipitation.

Infiltration is groundwater entering sewer lines through structural failures like cracks or defective joints (Environmental Protection Agency, 2004). It is governed by soil conditions, groundwater levels, precipitation, and infrastructure integrity. Infiltration occurs when the groundwater table is above a defective pipe (Fenner, 1990). Because groundwater recedes slowly, elevated infiltration can persist long after precipitation, chronically increasing sewer flow.

In North Carolina, 417 local government wastewater utilities were active as of December 2020 (Eskaf & Vulpis, 2021). Maintaining these systems requires substantial investment; the estimated 20-year capital cost for the state's water and wastewater infrastructure is \$17–\$26 billion (Durso et al., 2019). Delaying investment risks service degradation, public health, higher emergency repair costs, and lost economic opportunities.

Despite recognition of I&I as a major challenge, accurately identifying and quantifying its sources remains difficult. (Saletti, 2021) categorized existing methods into five groups: sensory methods, flow-based techniques, tracer approaches, I&I models, and emerging digital water tools.

These methods differ in scale, precision, and data requirements. Conventional techniques (e.g., CCTV inspection, smoke/dye testing) can indicate I&I presence and defects, but are labor-intensive, spatially limited, and often detect only partial sources. Advanced tools (e.g., tracer-based methods, hydraulic modeling) have improved diagnostics but are constrained by high cost and data availability.

This study hypothesizes that a fluorescence-based approach, tracking water's organic matter properties, can identify and quantify I&I source contributions in wastewater influent. Influent is the total flow entering the plant, which ideally is sanitary sewage but often includes I&I dilution. If confirmed, this offers a practical, scalable alternative for utilities to assess system performance.

The purpose of this study was to explore three main questions:

- How do differences in influent flow and dilution patterns among WWTPs reflect underlying variability in I&I dynamics?
- To what extent does antecedent precipitation influence dilution magnitude and the relative contributions of I&I sources in influent?
- Are there significant differences in I&I source contributions across facilities, specifically between Coastal Plain and Piedmont WWTPs?

These questions also evaluate the fluorescence-based method's performance and the broader hydrological/infrastructural patterns influencing I&I across North Carolina. Findings should offer insights for targeted infrastructure assessment, planning, and investment.

This approach could position fluorescence-based monitoring as an accessible method for quantifying I&I sources, benefiting small or underserved communities lacking resources for conventional monitoring. Stakeholders (e.g., WWTP operators, agencies, planners) could use this to support infrastructure assessments, guide investments, and enhance environmental monitoring.

2. Materials and Methods

2.1. Study sites and sample collection

The WWTPs in this study represent diverse state conditions (Table 1), varying in age, scale, and upgrade history. Table 1 lists initial construction year, sewer line length, and last major upgrade date. In coordination with the NC Department of Health and Human Services (DHHS), 24-hour composite influent samples were received twice weekly from each facility (22 Feb - 28 Oct 2024). Samples arrived in 125 mL amber HDPE bottles, cleaned with Sparkleen 1 detergent and rinsed with ultrapure water (MilliQ, 18.2 MΩ). This study involved ten NC WWTPs (Fig. 1): Jacksonville, Roanoke Rapids, Greenville, Wilson, Buncombe, Marion, McDowell Creek, Irwin Creek, Mallard Creek, and Sugar Creek (Table 2).

Metadata provided with each sample included influent flow rate, temperature, pH, and composite start/end times. Occasional gaps were noted. Precipitation data (mm/day) from the weather station closest to each WWTP were obtained from the North Carolina State Climate Office. These stations provided representative daily rainfall data to analyze relationships between antecedent precipitation and influent dilution.

Table 1. Key infrastructure characteristics of the WWTPs in this study include the year of initial construction, the length of sewer lines, and the date of the last major upgrade. Data obtained from the North Carolina Department of Environmental Quality's Wastewater Discharge Permitted Facilities database (accessed October 5, 2025). Available online: https://ncdenr.maps.arcgis.com/apps/webappviewer/index.html?id=4ca77e79b68e466cbcae9713a28dde7d

Facility	Year of construction	Year of Last Major Upgrade	Sewer System Characteristics
Buncombe County	1967	1980	1,157 miles of sewer line; 34,700 manholes
Greenville	1985	1995	539 miles; 44 pump stations
Irwin Creek	1927	Not reported	Not available
Jacksonville	1998	Not reported	300 miles
Mallard Creek	1979	Not reported	Not available
Marion	1978	2008	85 miles
McDowell Creek	1979	Not reported	Not available
Roanoke Rapids	1963	1983	146 miles; 6 pump stations; oldest pipes from 1930s
Sugar Creek	1927	2018	Not available
Wilson	1974 (First permit issued)	2004	358 miles; 4 pump stations

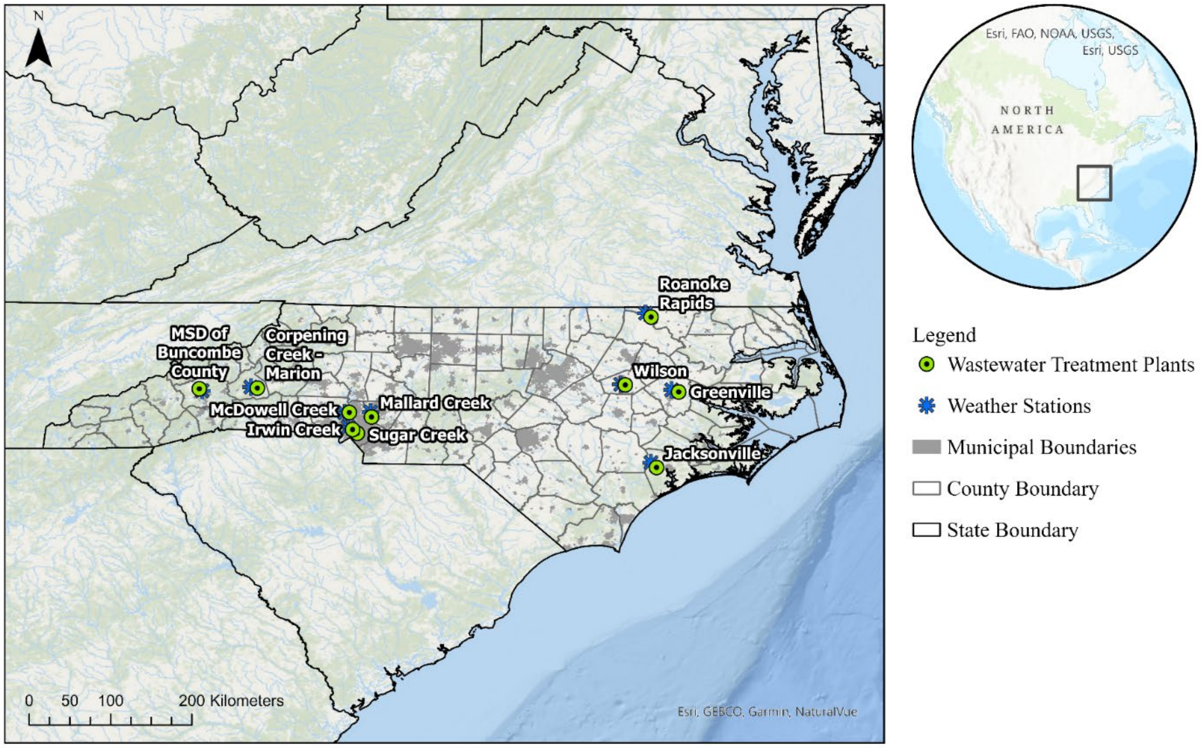

Figure 1. Geographic distribution of WWTPs and weather stations involved in this study.

Table 2. Participating WWTPs locations, populations served, and summary of sample collection details.

Municipality	Facility	Population served	Start date (2024)	End date (2024)	Total samples
Buncombe County	MSD of Buncombe County WWTP	173,000	26 April	13 Sep	40
Greenville	Greenville Utilities Commission WWTP	89,616	12 April	27 Aug	33
Charlotte	Irwin Creek WWTP	82,158	16 May	28 Oct	38
Jacksonville	Jacksonville Wastewater Facility	41,819	23 Feb	29 Oct	35
Charlotte	Mallard Creek WWTP	120,000	16 May	28 Oct	41
Marion	Corpening Creek WWTP	8,459	22 April	28 Oct	37
Charlotte	McDowell Creek WWTP	68,685	16 May	28 Oct	42
Roanoke Rapids	Roanoke Rapids Sanitary District	14,320	29 Feb	29 Oct	62
Charlotte	Sugar Creek WWTP	182,501	16 May	28 Oct	43
Wilson	Hominy Creek Wastewater Facility	52,000	12 Feb	28 Oct	73

Five-day antecedent precipitation (AP_5) was calculated as the sum of daily precipitation for the five days preceding sampling. This window reflects hydrological reasoning on sewer system response times, as I&I sources often exhibit lagged responses. Rainfall-derived I&I reaches monitoring points with a basin response lag due to travel time through soils or infrastructure

(Wright et al., 2001). (Flood & Cahoon, 2011) found rainfall integrated over three or more days accounted for most infiltration-related flow increases in coastal NC. As this study includes coastal plain and Piedmont WWTPs, a five-day window was selected to accommodate longer travel times and variable system responses across diverse hydrogeologic settings across a range of sewershed sizes.

Field collections characterized potential I&I sources. Groundwater samples were collected from USGS monitoring wells along the Rocky Branch stream (NCSU campus), providing a time series coincident with WWTP collections. Rainwater was collected periodically using a funnel and polycarbonate bottle in open residential areas (Raleigh, NC), capped, stored dark, and taken to the lab within 24 hr. Street runoff was sampled directly from storm drains in Raleigh during and after rain events. Samples were stored at 4°C. Nitrile gloves were used for all field samplings.

All laboratory materials and equipment for field sampling and for sample processing were cleaned with Sparkleen 1 detergent and rinsed with ultrapure water (MilliQ, 18.2 MΩ) prior to use.

2.2. Sample Preparation and Optical Analysis

All samples received by DHHS were pasteurized per its COVID surveillance program and stored at 4 °C until collected (average one week). Within 24 hours of receipt, wastewater samples were diluted 1:3 (vol/vol) to reduce suspended particles, then filtered through pre-combusted (450°C, 6 hours) Cytiva Whatman glass fiber filters (0.7 µm, GF/F). The filtrate was stored in polycarbonate bottles and refrigerated until analysis (within 4 days). I&I source samples were filtered and stored similarly.

Absorbance (Varian Cary 300 UV spectrophotometer) and fluorescence (Varian Eclipse spectrofluorometer) were measured on all filtered samples. Absorbance was measured from 200–800 nm (1 cm quartz cell). Samples with absorbance > 0.4 at 240 nm were diluted to minimize inner-filtering effects (Kothawala et al., 2013). Milli-Q water served as a blank. Blank-corrected absorbance was converted to Napierian absorption coefficients (α, m^{-1}) using Equation 1:

$$a_\lambda = \frac{A_{\lambda,sample} - A_{\lambda,blank}}{L}$$

where A is unitless absorbance, λ is the wavelength (nm), and L is pathlength of the quartz cell (m).

Fluorescence emission (Em) was measured (300–600 nm, 2 nm increments) and excitation (Ex) (240–450 nm, 5 nm increments). Lamp energy (voltage) was varied to keep sample emission responses <80% of signal maxima. Samples were diluted with ultrapure water as needed to match absorbance conditions. As for absorbance, an ultrapure water blank was subtracted from fluorescence measurements. Data were corrected for lamp energy, detector response, sample absorption, and dilution. Intensities were calibrated in quinine sulfate units (QSU; 1 QSU = 1 ppb quinine sulfate), following (Osburn et al., 2016). Post-processing used MATLAB (R2024b). For absorbance, Milli-Q spectra were subtracted, dilution corrections applied, and baseline offset/scatter corrected (referencing 750 nm).

2.3. Source Contribution Estimation

To estimate relative DOM source contributions, the regress-then-sum (RTS) method was applied. RTS – like other linear mixing models – assumes a mixed sample's fluorescence is a linear combination of known source profiles and is an application of generalized least squares regression (Bryan et al., 2023; Bryan et al., 2025). RTS updates the FluorMod framework, which previously required decomposing source EEMs via parallel factor analysis (PARAFAC) before fitting unknown samples (Osburn et al., 2016). With RTS, FluorMod no longer requires PARAFAC decomposition of the data (Bryan et al., 2023).

Using the RTS method, each unknown EEM was modeled as a non-negative linear combination of a reference dictionary comprising 64 published/validated EEMs and 78 new reference EEMs from this study (Osburn et al., 2016). These additions improve robustness and local representativeness, capturing study-specific conditions and objectives. RTS affords the flexibility to pre-define source categories based on prior knowledge of the system under study. For this project, the dictionary included 142 EEMs representing five potential I&I sources (rainwater, street runoff, soil leachate, groundwater, river water) and undiluted wastewater (Table 3).

All EEMs were vectorized, converting 2D matrices (excitation/emission axes) into 1D arrays by stacking emission values. Each EEM (151 Em x 43 Ex) was reshaped into a 6,493-element vector (6493 x 1). This enables standard math operations (e.g., matrix multiplication). The RTS method solves a non-negative least squares (NNLS) regression, regressing the unknown vectorized EEM against the full dictionary EEM matrix. The estimated regression coefficients indicate the relative strength of each reference EEM match. To obtain source-level estimates, coefficients are grouped by source category and summed (via a source-assignment matrix), producing a final vector. These weights represent the estimated DOM source contribution. To compare samples with different fluorescence intensities, the summed coefficients are reported as percentages per source. The RTS procedure was conducted in R using RStudio.

This modeling relies on the linear mixing hypothesis: a mixed DOM fluorescence profile is a weighted sum of its sources. This assumes conservative mixing (Hoff & Osburn, 2025), meaning spectral properties are preserved without significant alteration (e.g., microbial degradation, photodegradation, sorption). However, multiple examples per category provide insight into variation, possibly from environmental processes. The method also depends on a signal strong enough to resolve minor sources. When met, this is a validated approach for estimating DOM source contributions.

Table 3. Number of reference samples included in the dictionary by source category.			
Source Category	**Samples from Osburn et al., 2016, and Bryan et al., 2023**	**Samples collected in this study**	**Total number of samples in the dictionary**
Wastewater	13	25	38
Street runoff	20	21	41
Soil leachate	9	0	9
Groundwater	0	16	16
River	19	0	19
Rainwater	0	19	19

2.4. Model Fit Evaluation

To assess RTS model fit, the coefficient of determination (R^2) was calculated. A predicted EEM was generated for each sample by multiplying the NNLS-estimated weights by their corresponding vectorized reference profiles and summing the results. R^2 was calculated as:

$$R^2 = 1 - \frac{Residual\ sum\ of\ squares\ \ (RSS)}{Total\ sum\ of\ squares\ (TSS)}$$

where RSS is the squared difference (observed vs. predicted) and TSS is the squared difference (observed vs. mean). This quantifies how well the model reproduces the full fluorescence landscape.

2.5. Statistical Analysis

Statistical analyses and visualization were done in R (v. 4.4.1). Descriptive statistics (median, IQR, mean) summarized flow, dilution, and source contributions. AP5/flow relationships were evaluated (Pearson correlation). Kruskal–Wallis tests assessed source number differences (used for non-normal data, unbalanced sample sizes). The non-parametric Mann–Whitney U test (Wilcoxon rank-sum) compared groundwater contributions between regions. Groundwater was selected as high water tables define the Coastal Plain and are a hypothesized driver of regional I&I differences. Significance was set at $p < 0.05$. Boxplots illustrated distributions (median, IQR, 1.5× IQR whiskers, outliers, and '×' for means). Scatterplots and time-series plots showed correlations among AP5, flow, and composition.

3. Results

3.1. Preliminary Validation of FluorMod: Fluorescence-Based Source Apportionment Method

To support the FluorMod model's application in field conditions, controlled laboratory analyses evaluated how dilution and source mixing influenced fluorescence signals. These experiments were designed to verify the model's reliability and quantitative accuracy.

First, to test if dilution affects fluorescence-based source identification, it was hypothesized that reducing sample concentration would decrease overall fluorescence intensity without altering the underlying spectral characteristics. If the spectral shape remains intact, FluorMod should still attribute nearly 100% of the signal to wastewater, even at lower concentrations. This hypothesis was evaluated using a dilution series of two wastewater influent samples from Corpening Creek WWTP in Marion, NC, and Greenville, NC, WWTP, prepared in ultrapure Milli-Q water at concentrations of 70%, 55%, 40%, 25%, 10%, 5%, and 2.5%, with three replicates. Milli-Q water was used as a blank, leaving wastewater as the only source of fluorescent organic matter.

Across a range of dilution levels, modeled wastewater fractions remained nearly 100% (Fig. 2), particularly at influent concentrations above 10%, confirming the hypothesis that dilution reduces signal intensity without altering key spectral features. This is further supported by EEMs (Fig. 3), which show consistent fluorescence patterns across all concentrations, with only the intensity decreasing. The similarity in EEM shape demonstrates spectral structure is preserved even under strong dilution, validating FluorMod's capacity to attribute fluorescence to the correct source, even at low signal strength. Increased variability was observed at 5% or lower, where modeled contributions began to deviate from 100% to as low as 50%. Based on these results, a limit of detection (LOD) of 5% was established, reflecting the lowest concentration at

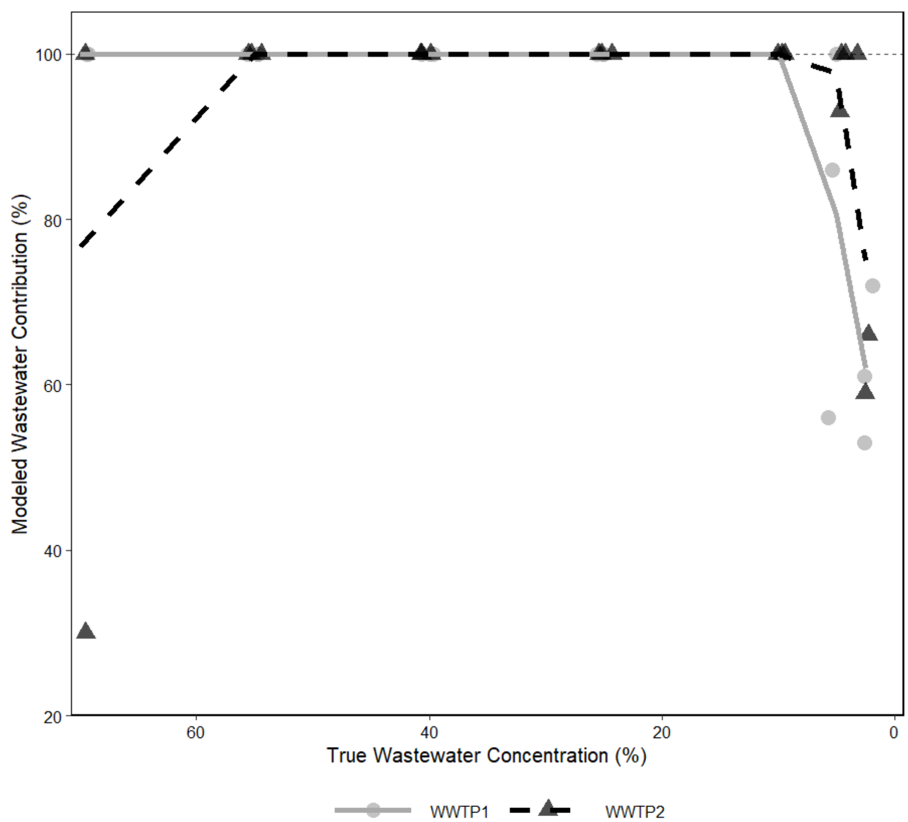

Figure 1. Modeled wastewater percentages estimated by FluorMod plotted against the known wastewater concentrations used in the dilution series. Wastewater samples, collected as 24-hour composites from Greenville (WWTP1) and Corpening Creek in Marion (WWTP2). Dilutions were made using ultrapure Milli-Q water.

which source attribution remains reliable. This threshold aligns with criteria from (Hoff & Osburn, 2025).

To further evaluate quantitative accuracy, controlled mixtures were prepared using three endmember water sources: groundwater from a residential well in Wake County, North Carolina; stream water from Rocky Branch Creek near NC State's campus; and wastewater from the Corpening Creek WWTP in Marion, NC. Representative EEMs (Fig. 4) showed distinct fluorescence patterns, consistent with previous work classifying signals into humic-like (peak A, peak C) and protein-like groups (Coble, 2007).

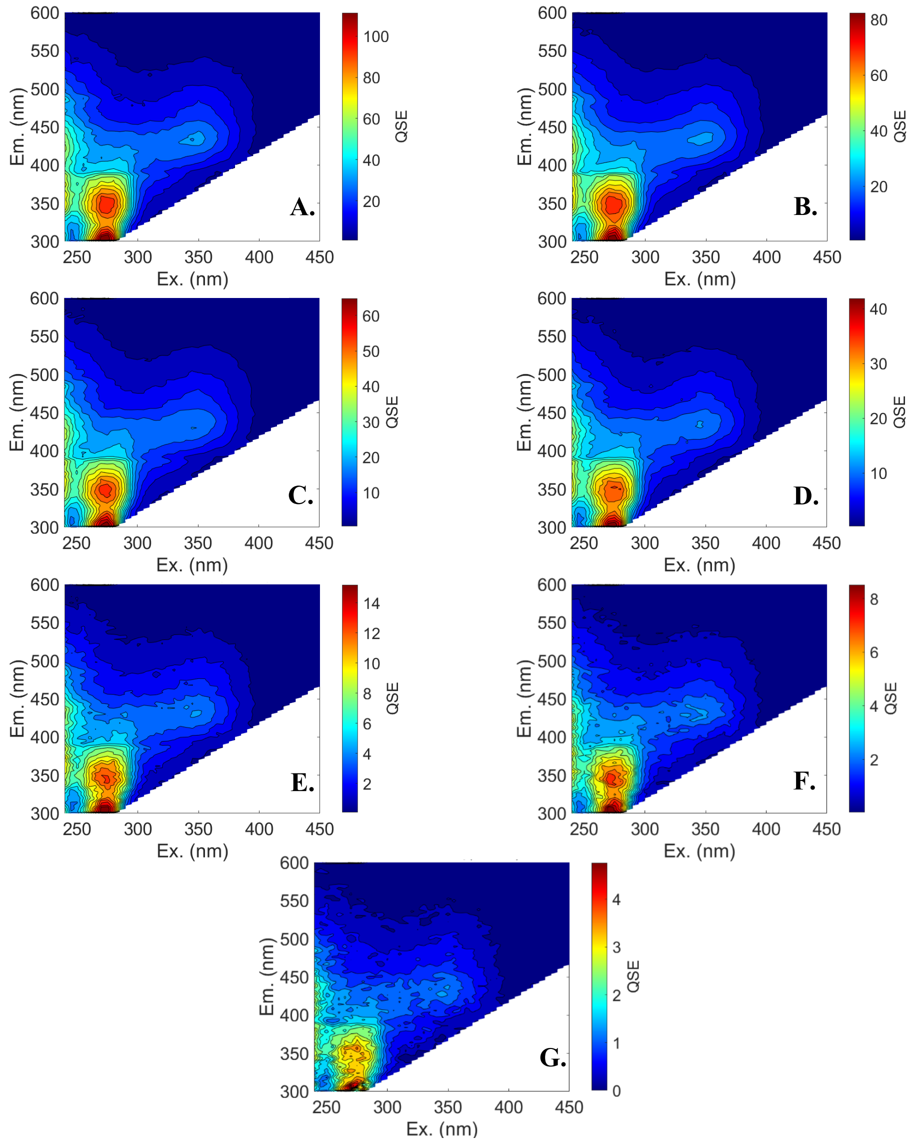

Figure 2. Representative EEMs from dilution experiment using a 24-hour composite wastewater sample from Greenville WWTP. Excitation (Ex) and emission (Em) wavelengths are in nanometers (nm), with fluorescence intensity reported in QSE. Note the differences in QSE scaling on the color bar for each EEM. Panels correspond to Wastewater concentrations in the dilution series: **(A)** 70%, **(B)** 55%, **(C)** 40%, **(D)** 25%, **(E)** 10%, **(F)** 5%, and **(G)** 2.5%.

Groundwater displayed minimal fluorescence (<1 QSE), with no clearly defined peaks – only faint traces of fluorescence (ca. 0.6 QSE) in the peak A region. Stream water exhibited stronger humic-like fluorescence, with contributions from both Peak A and Peak C (Ex=320–360/Em=420–460 nm), the latter often associated with terrestrial and anthropogenic inputs. Peak A is a signal common to streams and rivers, as well soils. Wastewater was dominated by protein-like fluorescence, with pronounced peaks corresponding to Peak B (tyrosine-like, Ex=275/Em=300–315 nm) and Peak T (tryptophan-like, Ex=275/Em=340 nm). Both tyrosine and tryptophan are fluorescent amino acids.

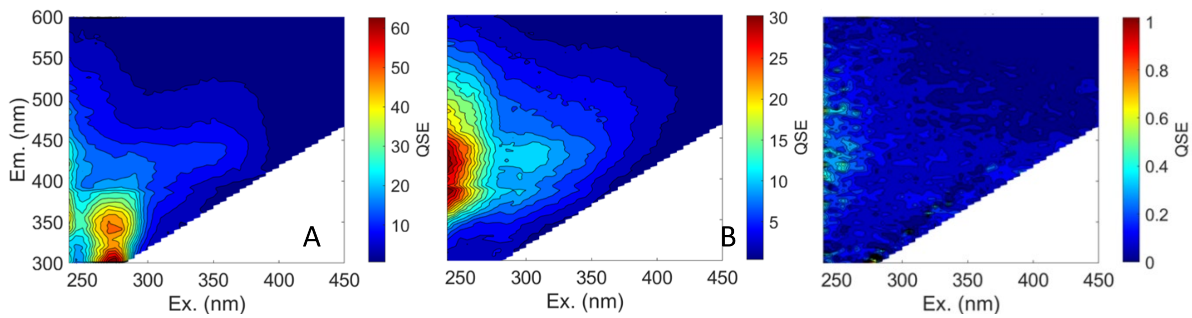

Figure 3. Representative EEMs of three endmember sources used in the mixing experiment. **(A)** Wastewater **(B)** Stream water and **(C)** Groundwater. Excitation (Ex) and emission (Em) are in nanometers (nm); fluorescence intensity is in quinine sulfate equivalents (QSE).

Seven mixing ratios were tested (Table 4), each in triplicate, to evaluate whether the EEM of each mixture corresponded to the weighted sum of its components. Each triplicate series was prepared and analyzed independently (reproduced three times daily). This design scheme provided experimental replication, allowing assessment of reproducibility and quantification of uncertainties.

Table 4. Mixture fractions of the three end-member water sources used in the controlled mixing experiment. 's' denotes source samples, where s1 = groundwater, s2 = stream water, and s3 = wastewater. 'm' denotes mixture samples composed of the three sources in the proportions shown.

Sample code	Groundwater	Stream water	Wastewater
s_1	1.00	0.00	0.00
s_2	0.00	1.00	0.00
s_3	0.00	0.00	1.00
m_1	0.00	0.50	0.50
m_2	0.50	0.50	0.00
m_3	0.50	0.00	0.50
m_4	0.25	0.25	0.50
m_5	0.25	0.50	0.25
m_6	0.50	0.25	0.25
m_7	0.33	0.33	0.33

Each replicate of the three source waters was treated as an independent endmember, and the model was applied across the full experimental dataset. The hypothesis was that FluorMod would accurately resolve source contributions in mixtures by representing each mixed sample as the weighted sum of its endmember EEMs. It was expected that modeled contributions for wastewater, stream water, and groundwater would correspond closely to their true mixing proportions, provided each endmember exhibited distinct, detectable fluorescence signatures.

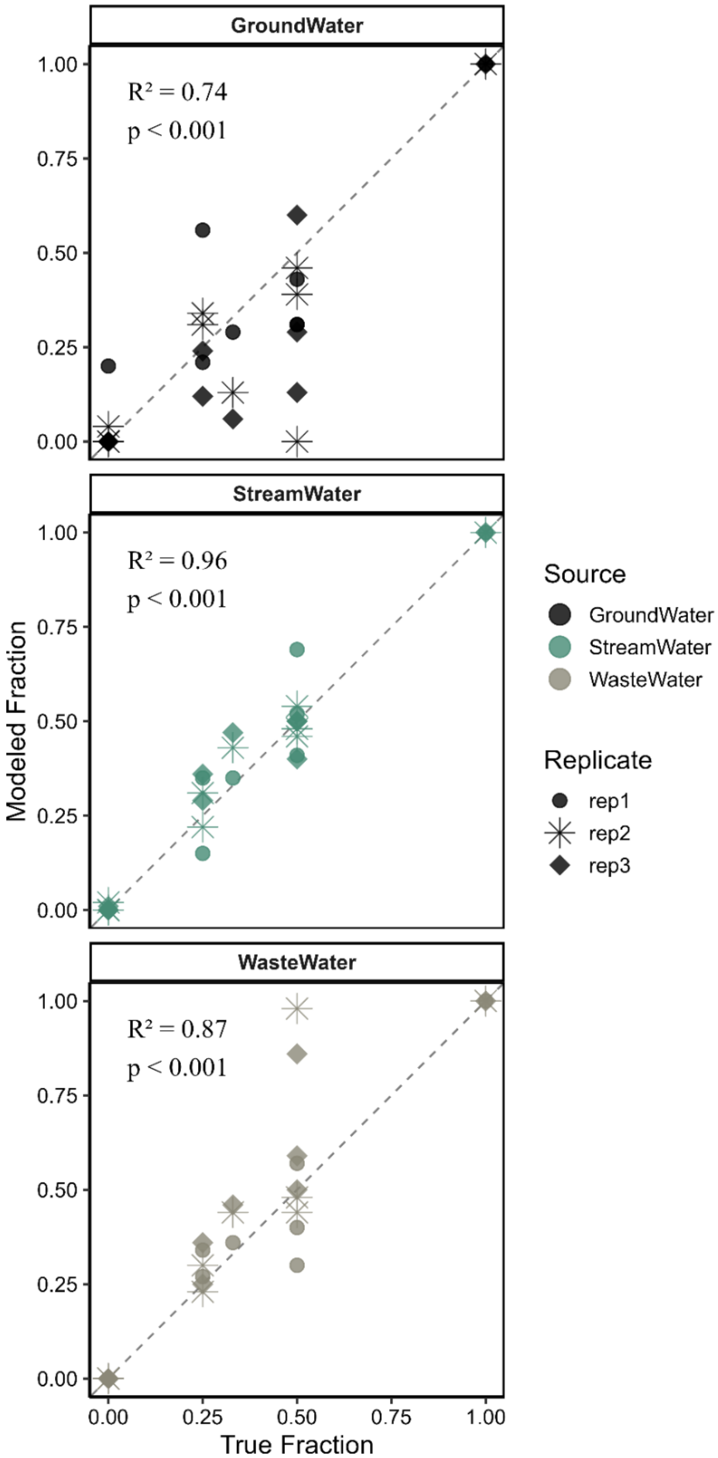

Figure 5. Regression plots comparing true versus estimated source contributions for seven different mixing arrangements using groundwater, stream water, and wastewater as end members.

Modeled source contributions for stream water and wastewater were highly consistent with the true proportions, with coefficients of determination (R^2) of 0.96 and 0.87, respectively (Fig. 5).

Replicate estimates were tightly clustered around the 1:1 reference line, indicating strong model performance. These results suggest the model can accurately estimate mixing proportions when endmembers have distinct, strong fluorescence signatures. In contrast, groundwater estimates showed greater variability among replicates and an R^2 of 0.74, suggesting lower precision.

These results show FluorMod is a robust, quantitative approach for source mixing. It provides reliable estimates of source contributions when endmembers are above the 5% detection limit and have distinct fluorescence signatures. The method is applicable across a range of source types and fluorescence intensities, with limitations only when signals approach background levels.

Notably, even for the highest-fluorescent wastewater mixtures, this experiment revealed substantial scatter. This scatter could result from uncertainties in preparing mixtures, including pipetting errors. Such analytical errors may explain modeled fractions that were both greater than and well below the 1:1 line (Hoff & Osburn, 2025).

3.2. Influent Flow Variability Across Facilities

Influent flow values varied widely among WWTPs, illustrated by boxplots comparing magnitude and variability of flow rates (MGD) (Fig. 6). Because the data were not normally distributed, the median provides a robust measure of central tendency. Buncombe and Sugar Creek exhibited the highest median influent flow rates, at 18.7 MGD and 16.6 MGD, respectively. McDowell Creek had the lowest median flow rate, at 6.0 MGD.

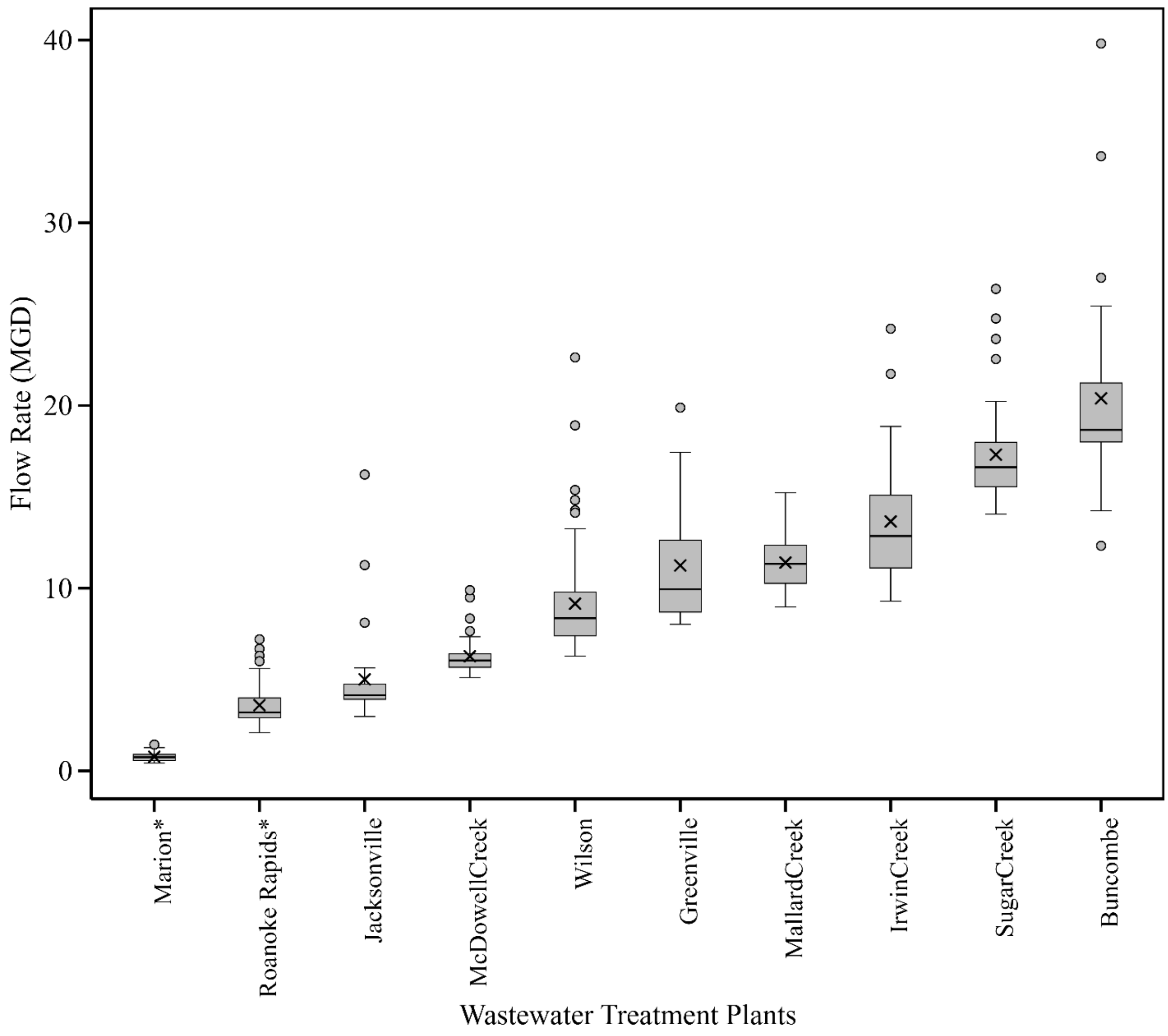

Figure 4. Influent flow rate in millions of gallons per day (MGD) across WWTPs. Boxes represent the interquartile range (25th to 75th percentiles), dark line indicates the median, and whiskers extend to values within 1.5× the interquartile range (IQR). Circles denote outliers, and the "×" symbol marks the mean flow rate for each plant. For WWTPs marked with an asterisk (*), effluent flow data were used as a proxy for influent flow.

The interquartile range (IQR) was calculated (Q3 – Q1) to quantify variability, as it suits skewed datasets with outliers (Table 5). The spread of the skewed results also varied. McDowell Creek and Jacksonville showed the narrowest IQRs for influent flow rate (0.7 and 0.8 MGD, respectively), suggesting consistent flow. In contrast, Irwin Creek and Greenville exhibited greater variability, with IQRs of 5.00 and 3.9 MGD, respectively.

Outliers (values > 1.5 times the IQR) were observed across most facilities and characterized as "high flow events," representing unusually large influent volumes. Buncombe and Sugar Creek displayed several high-flow events. Buncombe also displayed a low-flow outlier (12.3 MGD vs. 18.7 MGD median). Wilson showed multiple outliers, but with a moderate median (8.4 MGD) compared with Sugar Creek (16.6 MGD) and Buncombe (18.7 MGD). The highest flow at Wilson was 22.6 MGD (169% increase relative to its median). McDowell Creek (median: 6.1 MGD) also displayed high-flow outliers, illustrating that even plants with consistent baseline flows experienced episodic surges.

Distinct flow increases were observed at different times across facilities, often following multi-day rainfall accumulation. These rainfall–flow dynamics are illustrated in Appendices B–H. Early-spring (March) events at Roanoke Rapids and Wilson marked the first sharp increases in influent flow, followed by mid-spring (May) surges at Marion, Buncombe, and Irwin Creek (rainfall 50–100 mm). An increase occurred in July, when Buncombe, Irwin Creek, and Roanoke Rapids recorded influent peaks of 25-34 MGD after 80–100 mm of rainfall. Additional high-flow episodes in August and late September affected Greenville, McDowell Creek, Sugar Creek, and Wilson, associated with heavier antecedent rainfall (140–160 mm). Notably, August and late-September events likely reflect Tropical Storm Debby (August 3–8, 2024) (Reinhart et al., 2025) and Hurricane Helene (September 24–27, 2024) (Hagen et al., 2025).

Table 5. Summary statistics of influent flow rates across WWTPs. '*n*' indicates the number of samples. For WWTPs marked with an asterisk (*), effluent flow data were used as a proxy for influent flow

Facility	*n*	Min value	Max value	Median	Mean	Q1	Q3	Interquartile range (IQR)
Buncombe	37	12.3	39.8	18.7	20.4	18.0	21.2	3.2
Greenville	20	8.0	19.9	9.9	11.2	8.7	12.6	3.9
Irwin Creek	38	9.3	24.2	12.9	13.6	11.1	15.1	4.0
Jacksonville	27	3.0	16.2	4.1	5.0	3.9	4.8	0.8
Mallard Creek	41	9.0	15.2	11.3	11.4	10.3	12.4	2.1
Marion*	35	0.4	1.4	0.7	0.8	0.6	0.9	0.3
McDowell Creek	42	5.1	9.9	6.0	6.3	5.7	6.4	0.7
Roanoke Rapids*	62	2.1	7.2	3.2	3.6	2.9	4.0	1.1
Sugar Creek	43	14.1	26.4	16.6	17.3	15.6	18.0	2.4
Wilson	72	6.3	22.6	8.4	9.2	7.4	9.8	2.4

3.3. Antecedent Precipitation

Antecedent precipitation totals (AP_5) varied considerably across sampling events and facilities (Fig. 7). Given the skewed data, medians and IQRs summarized central tendency and variability (Table 6). Median AP5 values were generally low (< 10 mm), reflecting extended periods without rainfall. For example, Buncombe and Sugar Creek had medians of 7.0 and 2.8 mm, respectively, with narrow IQRs, indicating most sampling occurred during relatively dry conditions.

In contrast, Wilson and Roanoke Rapids exhibited greater variability (IQRs of 34.8 mm and 25.7 mm), indicating frequent transitions between dry and wet conditions. McDowell Creek also showed a broad IQR (26.0 mm), but its low median (6.2 mm) indicates most sampling occurred under relatively dry conditions, with the spread driven by occasional larger storms. Outliers (> 1.5 × IQR) corresponded to extreme rainfall events and were observed across several facilities, including Greenville, Irwin Creek, and Sugar Creek.

Overall, AP_5 distributions captured a spectrum of rainfall exposure conditions, from persistently dry baselines (e.g., Buncombe) to more precipitation-responsive catchments (e.g., Wilson and Roanoke Rapids). This variability provides essential context for interpreting how inflow and infiltration dynamics varied across facilities.

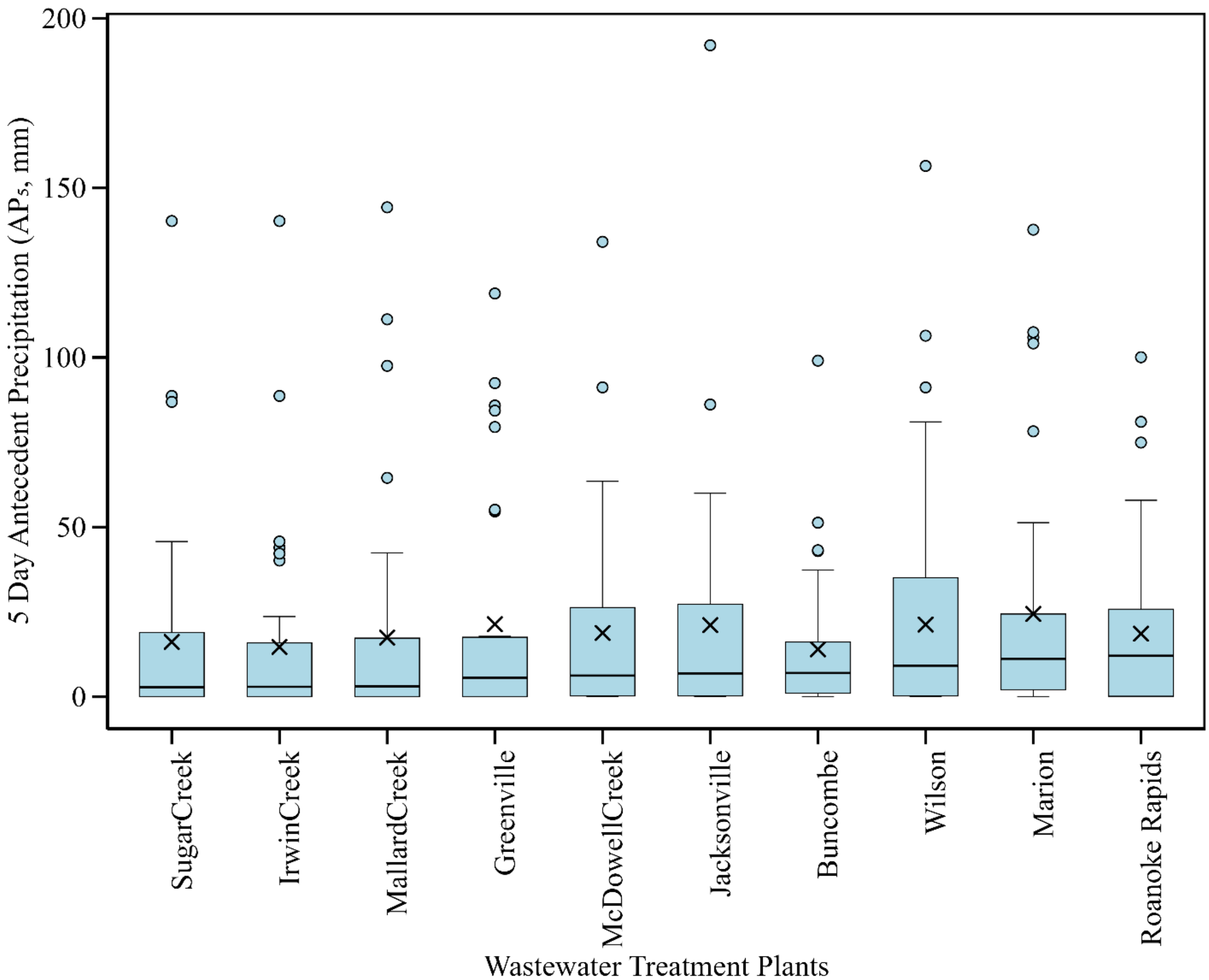

Figure 7. Antecedent precipitation totals (5-day cumulative, denoted as AP5 in millimeters) across WWTPs. Boxes represent the interquartile range (25th to 75th percentiles), dark line indicates the median, and whiskers extend to values within 1.5× the interquartile range (IQR). Circles denote outliers, and the “×” symbol marks the mean AP5 for each plant.

Table 6. Summary statistics of AP5 across WWTPs. n indicates the number of samples.

Facility	***n***	**Min value**	**Max value**	**Median**	**Mean**	**Q1**	**Q3**	**Interquartile range (IQR)**
Buncombe	40	0	99.1	7.0	14.0	1.1	16.1	15.1
Greenville	33	0	118.9	5.6	21.4	0.0	17.5	17.5
Irwin Creek	38	0	140.2	2.9	14.7	0.0	15.8	15.8
Jacksonville	35	0	192.0	6.9	21.1	0.3	27.2	27.0
Mallard Creek	41	0	144.3	3.0	17.4	0.0	17.3	17.3
Marion	37	0	137.7	11.2	24.4	2.0	24.4	22.3
McDowell Creek	42	0	134.1	6.2	18.8	0.3	26.3	26.0
Roanoke Rapids*	62	0	100.1	12.1	18.6	0.1	25.8	25.7
Sugar Creek	43	0	140.2	2.8	16.1	0.0	19.0	19.0

Wilson	73	0	156.5	9.1	21.2	0.3	35.1	34.8

3.4. Influent Dilution Distributions Across Facilities

The extent of influent dilution was examined to evaluate potential I&I across facilities. Boxplots visualized variability in influent composition (Fig. 8). Summary statistics are presented in Table 7. Influent dilution from I&I varied considerably among and within WWTPs. Several plants showed 0% median dilution (Buncombe, Mallard Creek, Marion, McDowell Creek, Sugar Creek), indicating little sustained I&I. In contrast, other facilities exhibited substantial dilution and broad variability (IQRs > 70%). This highlights significant differences among WWTPs, with some operating under stable conditions while others experience frequent, significant external input.

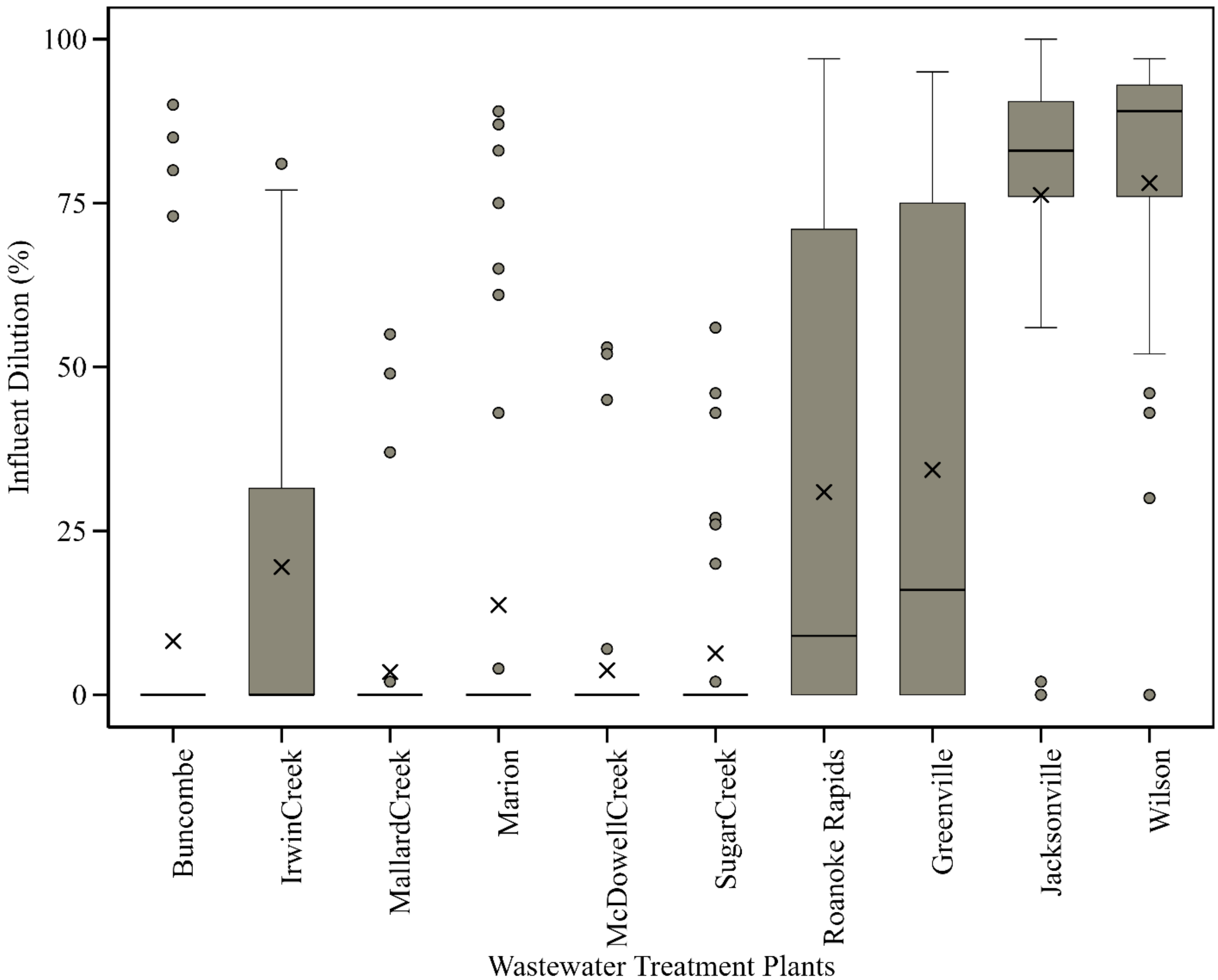

Figure 5. Influent dilution (%) across WWTPs. Boxes represent the interquartile range (25th to 75th percentiles), dark line indicates the median, and whiskers extend to values within 1.5× the interquartile range (IQR). Circles denote outliers, and the "×" symbol marks the mean.

In some cases, I&I effects were striking. Wilson had the highest median dilution (89% non-wastewater input), suggesting sustained I&I contributions. Roanoke Rapids and Greenville exhibited the highest variability (IQRs 71% and 75% respectively), indicating influent composition fluctuated substantially, alternating between no dilution and dominance by external sources. Irwin Creek also displayed considerable spread in dilution (IQR 31.5%). In contrast, the remaining facilities demonstrated lower I&I dilution (medians 0%–15%, IQRs 0%–32%), and experienced limited I&I influence and more stable influent compositions.

Table 7. Summary statistics of influent dilution percentages across WWTPs. n indicates the number of samples. For WWTPs marked with an asterisk (*), effluent flow data were used as a proxy for influent flow.

Facility	*n*	Min value	Max value	Median	Mean	Q1	Q3	Interquartile range (IQR)
Buncombe	40	0.0	90.0	0.0	8.2	0.0	0.0	0.0
Greenville	33	0.0	95.0	16.0	34.3	0.0	75.0	75.0
Irwin Creek	38	0.0	81.0	0.0	19.5	0.0	31.5	31.5
Jacksonville	35	0.0	100.0	83.0	76.2	76.0	90.5	14.5
Mallard Creek	41	0.0	55.0	0.0	3.5	0.0	0.0	0.0
Marion*	37	0.0	89.0	0.0	13.7	0.0	0.0	0.0
McDowell Creek	42	0.0	53.0	0.0	3.7	0.0	0.0	0.0
Roanoke Rapids*	62	0.0	97.0	9.0	30.9	0.0	71.0	71.0
Sugar Creek	43	0.0	56.0	0.0	6.3	0.0	0.0	0.0
Wilson	73	0.0	97.0	89.0	78.1	76.0	93.0	17.0

The presence of multiple outliers, particularly in facilities with low median dilution, highlights episodic dilution events. For example, Buncombe and Mallard Creek both had median dilution values of 0%, yet individual samples reached maximum dilutions of 90% and 55%, respectively. Similarly, Marion and McDowell Creek also showed episodic dilution, with maximum values of 89% and 53% despite medians of 0%. Even Sugar Creek, which generally exhibited stable conditions with a 0% median and IQR, recorded occasional dilution events up to 56%. These patterns clarify the distinction between WWTPs with a consistent, chronic I&I problem and those that were typically dominated by wastewater inputs but experienced substantial I&I during specific sampling events.

3.5. Influence of Precipitation on Influent Flow and Source Contributions

Time series analyses for each WWTP assessed how precipitation influenced influent flow volumes and composition. For each WWTP, AP_5 totals were compared with influent or (when unavailable) effluent flow rates. Relative contributions of individual sources (wastewater, groundwater, rainwater, river water, soil, street runoff) were examined. This approach enabled visual and statistical evaluation of how rainfall caused changes in flow and composition.

Flow responses to rainfall were quantified using Pearson correlation analyses of AP_5 flow rates with influent and effluent flow rates (Table 8). In facilities such as Marion and Roanoke Rapids, influent flow data were not available, and effluent flow rates were used as proxies. While this substitution introduces limitations, it still provides insight into overall system responsiveness.

The highest Pearson correlation coefficients were observed at Jacksonville ($r = 86$, $p < 0.001$), Sugar Creek ($r = 0.70$, $p < 0.001$), Buncombe ($r = 0.65$, $p < 0.001$), and Wilson ($r = 0.65$, $p < 0.001$), indicating rainfall events were closely followed by increases in influent volumes. The lowest Pearson correlation coefficient was at Marion ($r = 0.32$, $p = 0.088$), which was not statistically significant. This weaker relationship may be partly explained by the reliance on effluent data to estimate influent flow. The lowest significant Pearson coefficients were at Mallard Creek ($r = 0.49$, $p < 0.005$) and McDowell Creek ($r = 0.52$, $p < 0.001$), suggesting precipitation events had only a minimal direct impact on inflow rates. Example plots are presented for Wilson, Greenville, and McDowell Creek WWTPs (Fig. 9), with a complete set in Figure S1.

Table 8. Summary statistics of the correlation between 5-day cumulative precipitation and influent and effluent flow rates across WWTPs.

Facility	Input	Pearson correlation coefficient (r)	*p*-value
Buncombe	Influent flow	0.65	< 0.001
Greenville	Influent flow	0.57	0.009
Irwin Creek	Influent flow	0.60	< 0.001
Jacksonville	Influent flow	0.86	< 0.001
Mallard Creek	Influent flow	0.49	0.001
Marion	Effluent flow	0.32	0.088
McDowell Creek	Influent flow	0.52	< 0.001
Roanoke Rapids	Effluent flow	0.54	< 0.001
Sugar Creek	Influent flow	0.70	< 0.001
Wilson	Influent flow	0.65	< 0.001

Figure 9. Correlation between 5-day antecedent precipitation and influent rates. (Top) Wilson, (Middle) Greenville and (Bottom) McDowell Creek WWTPs

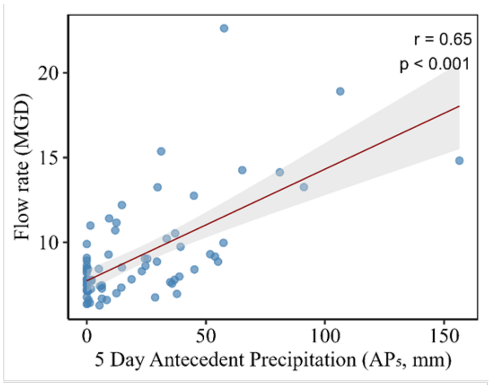

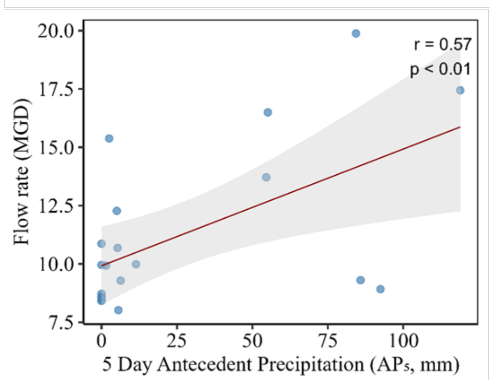

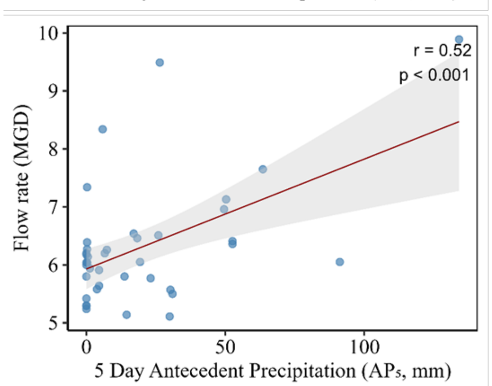

Time series plots illustrated the dynamics of influent source composition and flow in relation to precipitation (Figs.s 10 – 12). Three WWTPs —Buncombe, Wilson, and Irwin Creek —are presented. Buncombe WWTP was least affected by I&I. Influent flow rates responded to rainfall, but composition remained wastewater-dominated (median 100%). Only two events (May 10, July 19–26) exhibited measurable dilution (wastewater declining to 18%). In contrast, Wilson WWTP (most affected) exhibited consistent dilution (median 89%), with groundwater contributing significantly under dry and wet conditions. Irwin Creek showed an intermediate pattern. Wastewater dominated during dry periods (median 100%), whereas rainfall events ($AP_5 > 10$ mm) increased flow, greater source diversity, and dilution (wastewater declined to 80%).

Baseline conditions ($AP_5 < 10$ mm) were used to isolate dry-weather conditions (Table 9). Several facilities exhibited stable wastewater dominance, indicating minimal chronic I&I. These included Buncombe (all 25 dry samples 100% wastewater) and Mallard Creek (wastewater > 96% in nearly all samples). Marion similarly showed no detectable dilution in 15 dry-weather samples. McDowell Creek showed weak dilution effects (average 94% wastewater).

In contrast, other facilities showed persistent dilution. Wilson exhibited an average dilution of 77% under dry conditions, with groundwater as the dominant source (46% vs. 27% rainwater; other sources <4%) (Fig. 10). Irwin Creek exhibited an episodic pattern (average 14% dilution) (Fig. 12). Rainwater was the largest diluent (12% average) vs. groundwater (<2%). This reflects the overall trend, but the Irwin Creek time series (Fig. 11) suggests rainfall location plays an

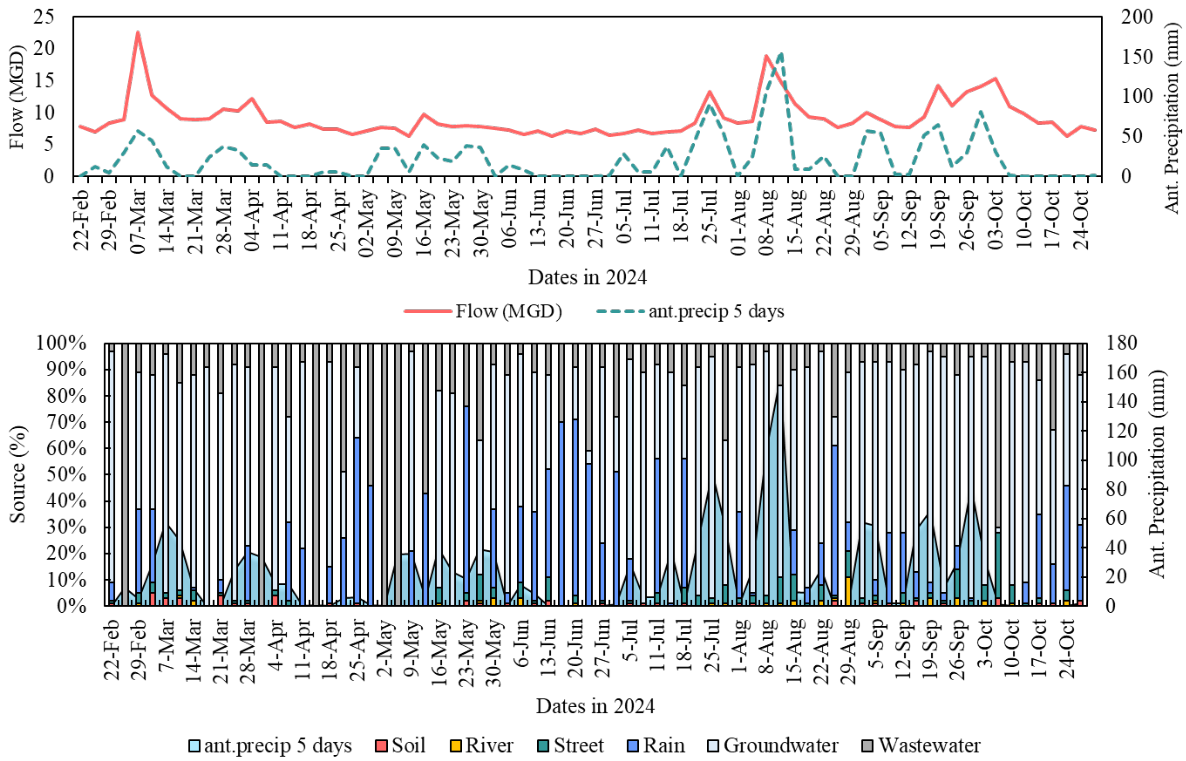

Figure 10. Influent flow, precipitation, and source contributions at Wilson WWTP. (A) Influent flow rates (million gallons per day, MGD) and antecedent 5-day cumulative precipitation (mm). (B) Relative contributions (%) of wastewater and other water sources to influent dilution over time.

important role in I&I dynamics.

Table 9. Summary of wastewater contributions under dry-weather conditions, defined as five-day antecedent precipitation <10 mm, across WWTPs. For each facility, the number of dry-weather samples (n), the average wastewater contribution (in percentage), and the minimum observed wastewater percentage.

Facility	*n* (dry-weather samples)	Avg % Wastewater	Min % Wastewater
Buncombe	25	100%	100%
Greenville	20	66%	14%
Irwin Creek	24	86%	19%
Jacksonville	19	22%	0%
Mallard Creek	40	96%	45%

Marion	15	100%	96%
McDowell Creek	24	96%	47%
Roanoke Rapids	29	85%	13%
Sugar Creek	27	96%	54%
Wilson	37	23%	3%

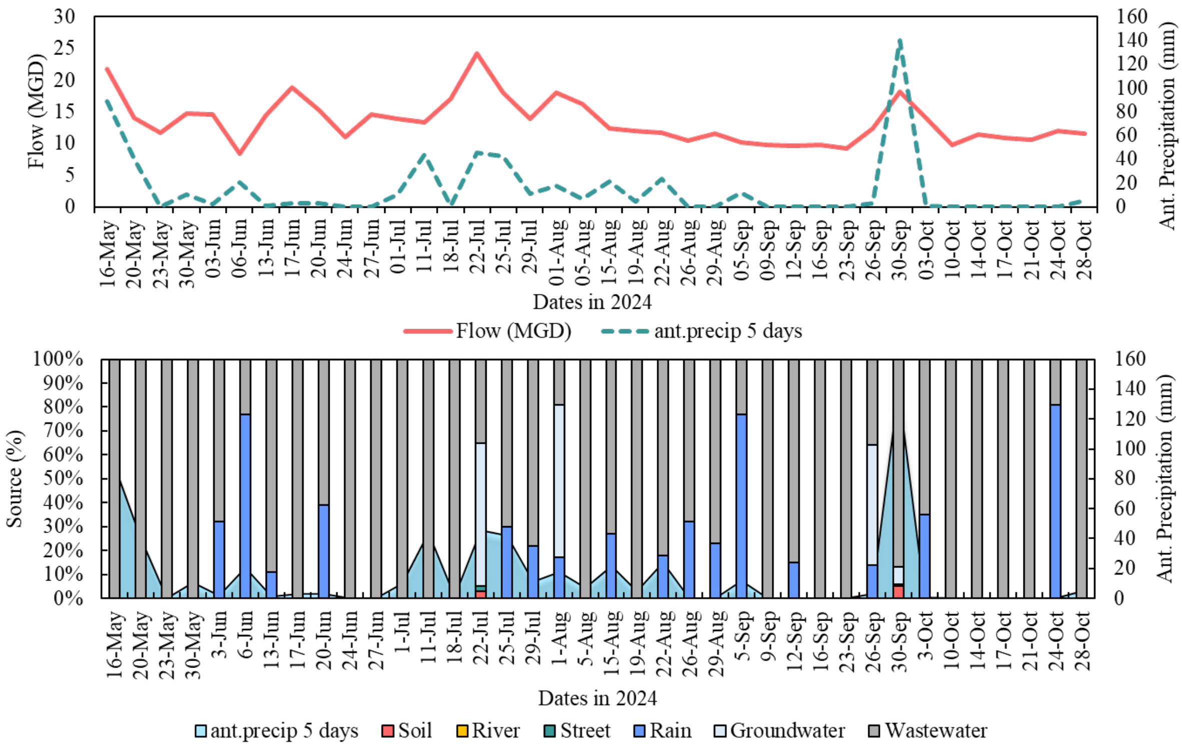

Figure 11. Influent flow, precipitation, and source contributions at Wilson WWTP. (A) Influent flow rates (million gallons per day, MGD) and antecedent 5-day cumulative precipitation (mm). (B) Relative contributions (%) of wastewater and other water sources to influent dilution over time.

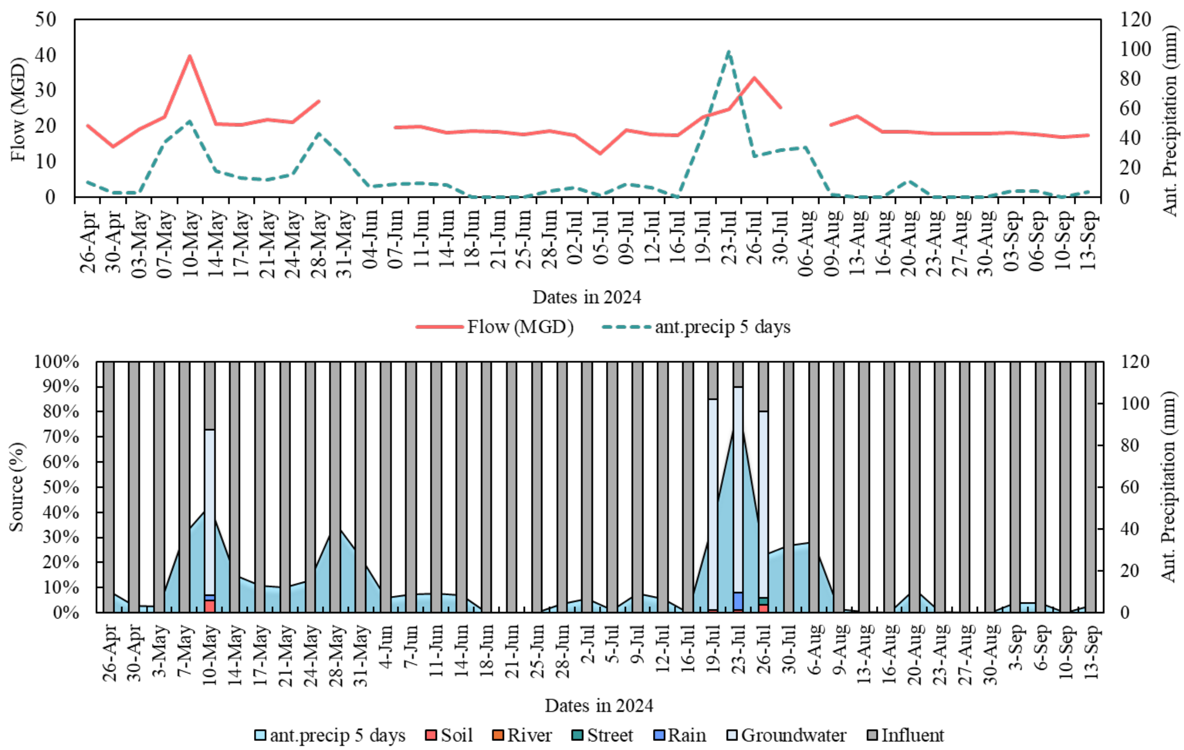

Figure 11. Influent flow, precipitation, and source contributions at Wilson WWTP. (A) Influent flow rates (million gallons per day, MGD) and antecedent 5-day cumulative precipitation (mm). (B) Relative contributions (%) of wastewater and other water sources to influent dilution over time.

3.5. Influence of Rainfall on I&I Source Diversity

To explore whether precipitation events also influenced the number of contributing sources, the number of external sources contributing to total influent flow was calculated for each sample. The highly skewed nature of precipitation (many small events, infrequent large events) data complicates strict quantile classification (von Storch & Swiers, 1999). Therefore, quantile-based binning into three categories (terciles) was applied after removing zero values. Bins corresponded to the following AP5 categories: Low: <10 mm, Moderate: 10–30 mm, and High: >30 mm. Boxplots compared this source diversity across the three precipitation categories for each facility. These final categories preserve the influence of heavy rainfall events and enable consistent comparison. Results showed that several facilities exhibited increases in source diversity with higher rainfall (Fig. 13).

A Kruskal–Wallis rank sum test was applied to these non-normal data of differing sample sizes. Results showed the number of contributing sources varied significantly among rainfall categories at Buncombe ($\chi^2 = 10.8$, $p = 0.005$), Greenville ($\chi^2 = 6.48$, $p = 0.039$), and Roanoke Rapids ($\chi^2 = 8.83$, $p = 0.012$). In these facilities, higher AP_5 values were associated with greater source diversity, indicating rainfall mobilized multiple I&I pathways. In contrast, no significant differences were detected at the remaining facilities ($p > 0.05$). Visual inspection of the boxplots highlights several notable patterns. Wilson and Jacksonville exhibited consistently higher median source counts across categories, reflecting chronic exposure to multiple contributing sources regardless of rainfall. In contrast, McDowell Creek, Mallard Creek, and Sugar Creek showed median I&I contributions near zero, indicating I&I contributions were rare and generally limited to episodic events.

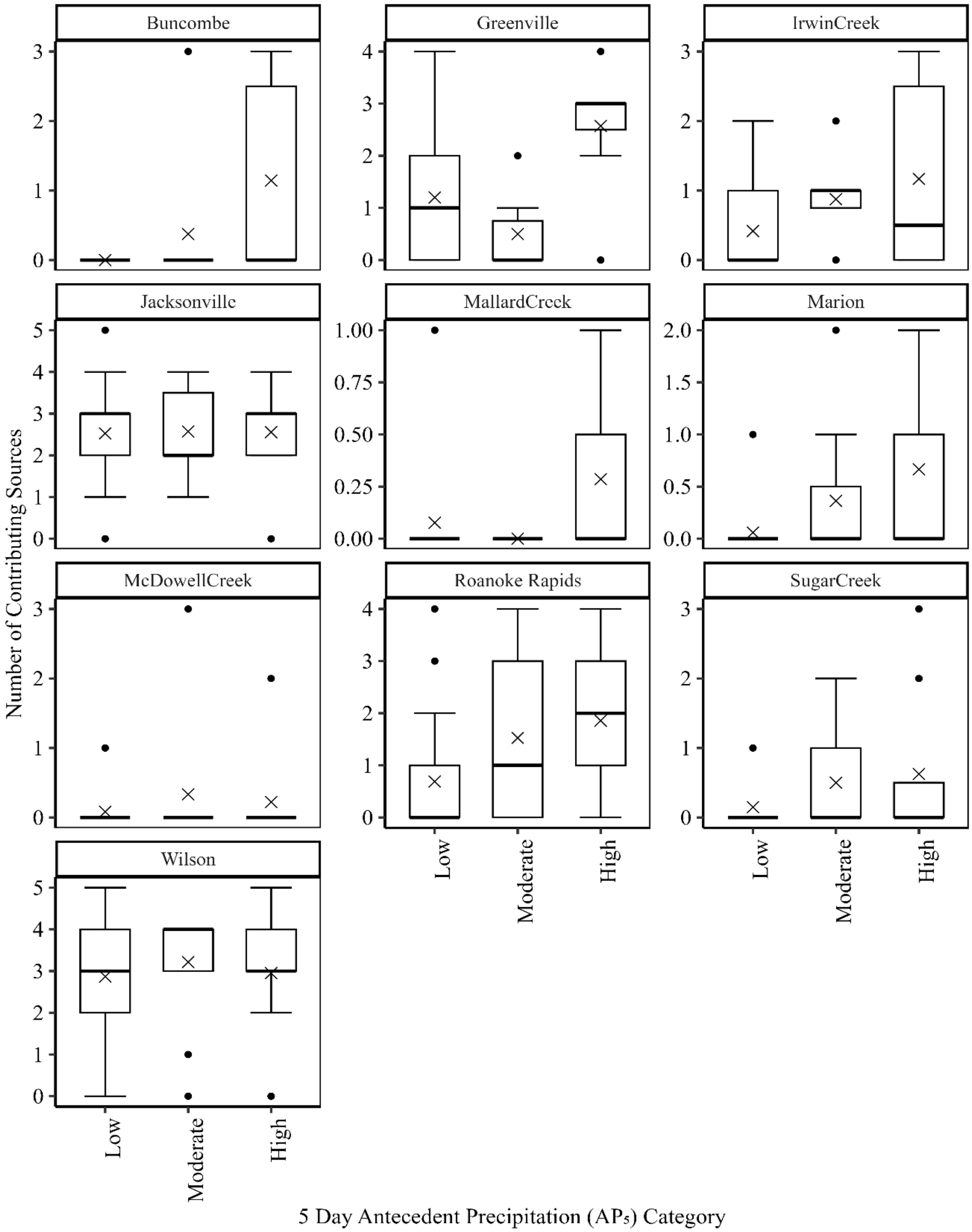

Figure 13. Boxplots showing the number of contributing sources to total influent across three AP_5 categories (Low: <10 mm, Moderate: 10–30 mm, High: >30 mm) for each WWTP. Boxes represent the interquartile range (25th to 75th percentiles), the dark line indicates the median, and the "×" symbol marks the mean. Whiskers extend to values within 1.5× the IQR and black circles represent outliers.

4. Discussion

4.1. Dilution Patterns Reveal Distinct I&I Regimes Across WWTPs

Marked differences in dilution dynamics indicated distinct I&I regimes. Based on temporal patterns and dilution magnitude, facilities were grouped into three representative categories. This classification, developed from the present dataset, aligns with previous observations that I&I contributions vary significantly among systems.

The first category (Wilson and Jacksonville WWTPs) exhibited consistently high dilution, independent of antecedent precipitation. This suggests chronic groundwater infiltration, a persistent dilution source. Prior work has shown that groundwater infiltration can account for 85% of total I&I, often irrespective of rainfall (Karpf & Krebs, 2011). Zhang and Parolari (2022) also demonstrated I&I can dominate sewer flow, exceeding dry-weather wastewater flows, particularly when sewer defects and shallow groundwater coincide.

The modeled I&I sources, summarized as a heat map, support this interpretation (Fig. 14). Wilson had the highest average groundwater contribution (56%) with rainfall at 18%, confirming groundwater infiltration dominance, likely due to shallow water tables in the Coastal Plain. Jacksonville showed a more balanced composition (37% rainfall, 34% groundwater, 5% street runoff), suggesting both direct stormwater inflow and groundwater intrusion are active pathways. These results reinforce that while both facilities experience chronic dilution, the dominant mechanisms differ: Wilson is groundwater-driven, while Jacksonville also receives stormwater inflow.

However, Wilson and Jacksonville deviated from seasonal I&I patterns reported in the literature. Groundwater infiltration is often characterized as seasonally modulated, responding to hydrologic cycles (Wittenberg & Aksoy, 2010). Their analysis of systems in Germany and Turkey showed intrusion behaves analogously to stream baseflow. WWTPs close to rivers where sewer lines were below the water table experience constant hydraulic pressure. Similarly, Sowby & Jones (2022) modeled seasonal fluctuations in Utah, finding groundwater contributions peaked in spring when most precipitation occurred, but remained year-round. Their results emphasized that groundwater infiltration was consistently present and dominant, reinforcing that saturated soils maintain infiltration if defects are present.

The persistent groundwater contribution identified for both WWTPs suggests that these systems are governed by a chronic infiltration regime rather than short-term rainfall events. This chronic infiltration may reflect long-standing hydraulic connectivity between shallow groundwater and the sewer network, exacerbated by aging infrastructure, fractured pipes, or sewer lines in saturated soil. Such sustained conditions indicate a continuous infiltration regime, not just a response to short-term inputs. This distinction implies conventional storm-related mitigation strategies may be insufficient. These systems likely require structural rehabilitation and targeted inspections to address this chronic dilution.

The second category (Greenville, Roanoke Rapids, Irwin Creek WWTPs) showed highly variable dilution, with wastewater percentages fluctuating considerably. The correlation between AP_5 and influent flow was moderate (Table 7), indicating rainfall only partially explained the variation. Under dry conditions, wastewater comprised 66% (Greenville), 85% (Roanoke Rapids), and 86% (Irwin Creek) of the influent (Table 8). Substantial dilution persisted, suggesting other factors.

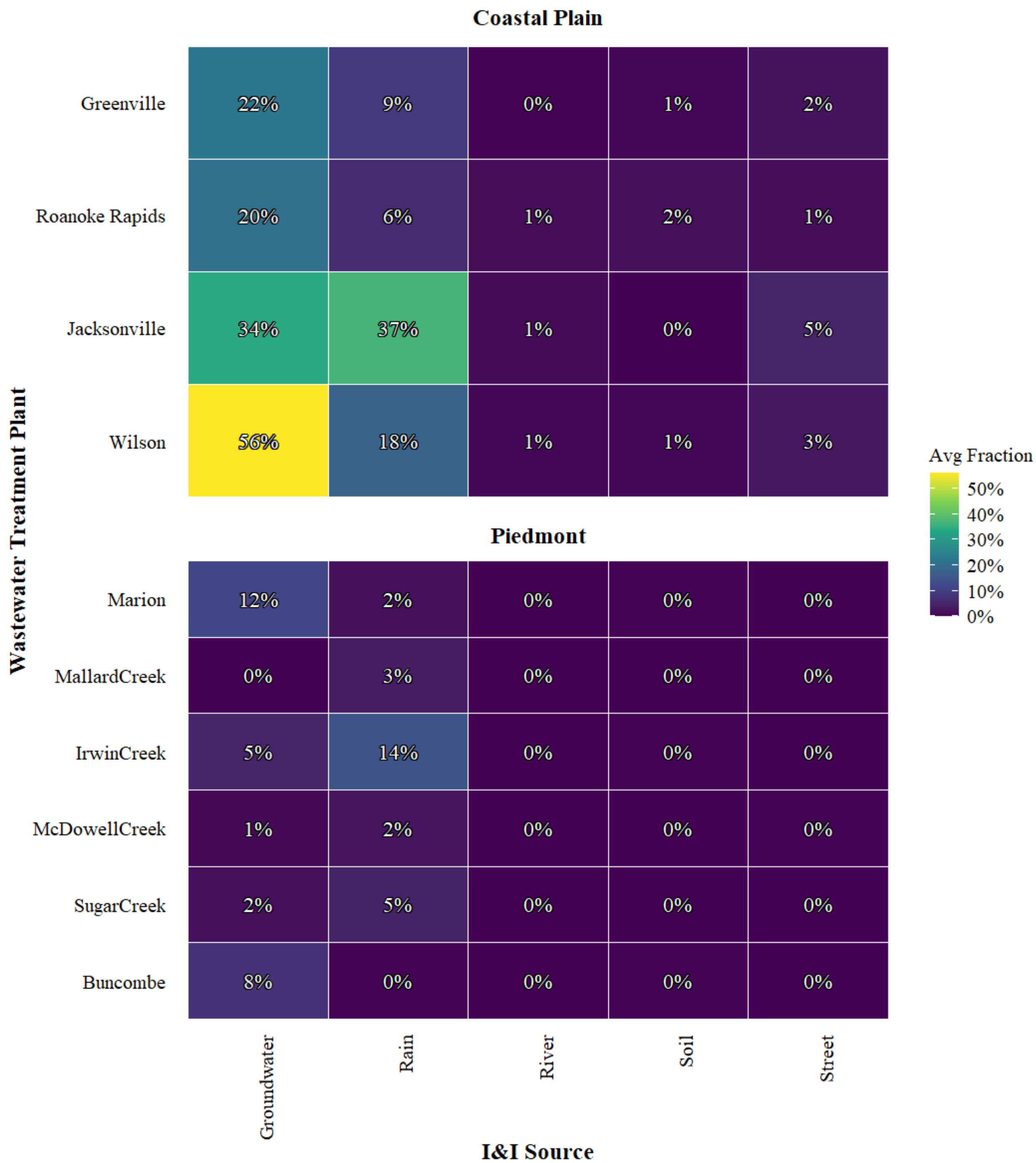

Figure 14. Average fractional contributions of non-wastewater sources (i.e., I&I) to total influent dilution across WWTPs in the Coastal Plain and Piedmont regions. Values represent the proportion of each I&I source: groundwater, rain, river, soil, and street runoff, as estimated by the FluorMod model. Percentages do not sum to 100%, as the remainder is attributed to wastewater. These values represent average source contributions to the diluted portion of the influent, based on all samples collected during the study period.

Average I&I source contributions (Fig. 14) support this mixed behavior. Greenville (22% groundwater, 9% rainwater) and Roanoke Rapids (20% groundwater, 6% rainwater) showed measurable groundwater and rainwater influence, indicating overlapping I&I mechanisms. This is not unique; (Cahoon & Hanke, 2017) reported over 40% of eastern NC systems had non-rainfall I&I components exceeding 10% of dry-weather flow. Similarly, groundwater infiltration persisted in a Norwegian municipality even during dry weather, although stormwater inflow dominated during wet weather (Roghani et al., 2024).

Kracht et al. (2007) used stable isotope tracers to distinguish between sources, estimating infiltrating groundwater contributed 39% of total dry-weather discharge. These findings support the FluorMod interpretation that Greenville and Roanoke Rapids operate under an intermediate I&I regime: responsive to rainfall yet sustained by structural pathways that continuously dilute influent with groundwater.

The third category (Buncombe, Mallard Creek, Marion, McDowell Creek, Sugar Creek WWTPs) exhibited the most resilient systems, with minimal influent dilution. This resilience was reflected in median dilution and IQRs of zero (Fig. 8, Table 7). In other words, dilution was absent during dry weather and only observed following rainfall events. Correspondingly, median wastewater contributions under dry conditions exceeded 96% at all five facilities (Table 9).

This dilution result is consistent with source contributions indicating very low rainwater fractions (≤ 5%) (Fig. 14). Irwin Creek was an exception at 14%. Groundwater contributions were also minimal, though Buncombe (8%) and Marion (12%) were slightly higher than other WWTPs. Dilution was episodic, showing a moderate positive correlation with AP_5 ($r = 0.49$–0.70; Table 8). Unlike systems with chronic infiltration or mixed responses, these WWTPs do not experience persistent dry-weather dilution. Instead, infiltration occurs only following precipitation, suggesting groundwater's entry is contingent on prior rainfall. The connection to groundwater is not continuously active but becomes engaged when precipitation raises the water table or saturates the soil (Staufer et al., 2012).

Overall, integrating dilution dynamics with modeled I&I source contributions provides a coherent framework that supports the central hypotheses of this study. The heat map results demonstrate that facilities located in the Coastal Plain are dominated by persistent groundwater infiltration, consistent with the influence of shallow water tables and saturated soils. In contrast, Piedmont systems are characterized by I&I occurring primarily after precipitation events. Intermediate systems such as Greenville and Roanoke Rapids exhibit mixed source behavior, confirming that both groundwater and rainfall contribute to variable but continuous dilution patterns.

4.2. Influence of Geographic Setting on I&I Dynamics

Geographic setting appears to be a major control on the observed differences in I&I contributions between facilities in the Coastal Plain and those in the Piedmont region (Fig. 15). WWTPs in the Coastal Plain (Wilson, Greenville, Roanoke Rapids, Jacksonville) exhibited substantially higher dilution and more groundwater contributions than those in the Piedmont (Buncombe, Mallard Creek, McDowell Creek, Irwin Creek, Marion, Sugar Creek). These patterns indicate that geology, groundwater table behavior, slope, and hydraulic connectivity are critical in governing infiltration processes.

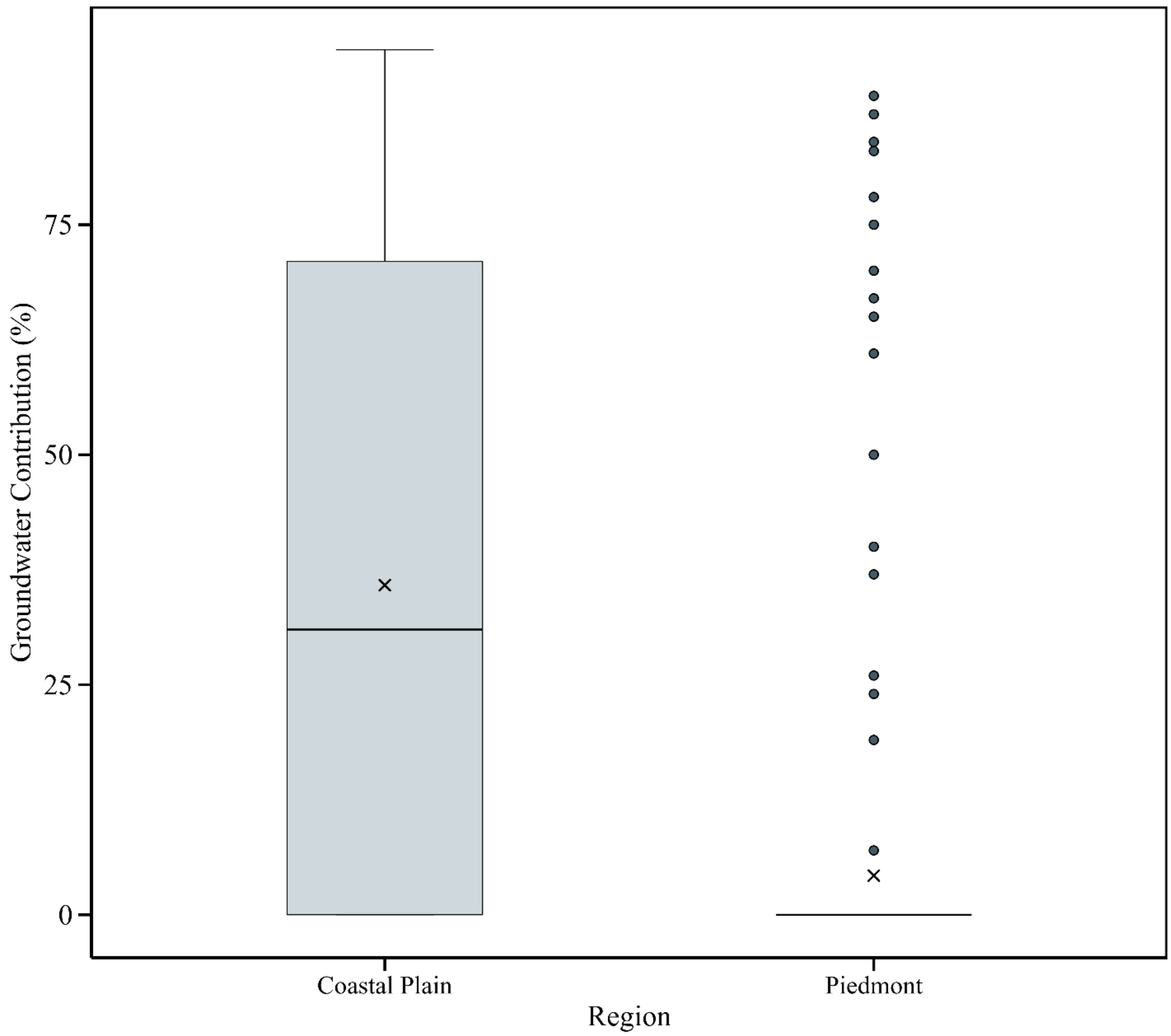

Figure 15. Groundwater contribution (%) to influent composition at WWTPs in the Coastal Plain and Piedmont of North Carolina. Boxes represent the interquartile range (25th–75th percentiles), the dark horizontal line indicates the median, and the "×" symbol marks the mean. Whiskers extend to the most extreme values within 1.5× the IQR, while circles denote outliers.

Coastal Plain areas tend to be flatter, underlain by shallow, often phreatic aquifers, and have soils that remain highly saturated near ground level. In such settings, sewer lines are more likely to intersect or lie close to areas where groundwater can enter pipes, due to the hydrostatic pressure. Damaged or otherwise compromised infrastructure worsens the problem. Working in low-lying areas of Belgium, Dirckx et al. (2016) found that groundwater infiltration is generally more pronounced in flat terrain with high water tables. In contrast, hilly or mountainous regions having steeper slopes and deeper groundwater reduce sustained hydraulic contact with sewer infrastructure. Similarly, in eastern North Carolina, widespread and significant groundwater infiltration into the sewage collection system often exceeded surface inflows, particularly in the Coastal Plain (Cahoon & Hanke, 2017).

Coastal vulnerability also comes from sea level rise. In Pearl City, HI, sea level rise exacerbated groundwater infiltration into sewer systems, leading to chronic I&I even during dry periods, due to the persistent pressure on sewer infrastructure (Budd et al., 2020). Thus, sea level rise can sustain high groundwater levels and create persistent infiltration pressure on sewer infrastructure not designed to withstand such pressure. For example, Rossi & Toran (2019) used historical census and GIS data from tidal Philadelphia, PA, to examine the relationship between early 20th-century sewer infrastructure and groundwater behavior. They found that aging sewer systems are highly susceptible to elevated groundwater pressures and sustained infiltration, driven by rising sea levels and shifting hydrologic patterns. They noted that this situation is a consistent problem across many U.S. coastal cities, where historic sewer networks intersect with shallow, tidally influenced aquifers.

Finally, (Zeydalinejad et al., 2024) synthesized findings from 83 peer-reviewed studies and concluded that groundwater infiltration is widespread across sewer networks globally, even in the absence of surface flows. While seasonal fluctuations are often observed, a persistent component of groundwater infiltration remains present year-round. They emphasized that baseline infiltration is a common feature, particularly in areas with shallow water tables or aging infrastructure – clearly a common theme found in the present work.

4.3. Increase in Contributing Sources with Rising Antecedent Precipitation

Antecedent precipitation influenced the diversity of I&I sources across facilities, although the strength of this relationship varied considerably. At Buncombe, Greenville, and Roanoke Rapids WWTPs, the number of contributing sources increased under high AP_5 conditions (Fig. 13). This pattern indicates that rainfall activates additional I&I pathways into sewer networks.

AP_5 is a useful metric because it integrates rainfall over several days. As a proxy, AP5 represents soil saturation and rising groundwater levels, key conditions that create infiltration pathways. An uncertainty is rainfall intensity, which may highlight rapid inflow sources, such as roof downspouts or misconnected gutters, compared to slower subsurface flow paths. For example, (Choi & Schmidt, 2020) modeled three I&I sources: downspouts, sump pump, and leaky laterals, each with distinct temporal signatures depending on how fast water moves through different media. Leaky laterals refer to aging or damaged private sewer pipes that connect individual properties to the main sewer line and allow groundwater or infiltrated stormwater to enter the system. In heavy storms, fast-response pathways may dominate. During steady rain, slower percolation flows may contribute more gradually, resulting in a lag between rainfall and detectable dilution in the sewer system.

The spatial distribution of precipitation across the sewershed also matters in I&I response. Rainfall estimates can vary significantly depending on how precipitation is measured or interpolated across a catchment, with large effects on modeled I&I flows (Wride et al., 2004). Spatial variability likely explains cases in which AP_5 occurred but no clear impact on I&I was detected. For example, in early spring in Greenville (Fig. S2, Fig. 2) and in McDowell (Fig. S2, Figs. 1 and 2) in early September, influent flow remained unchanged, and no dilution was observed despite AP_5 values reaching 60 mm. Thus, rainfall may have occurred outside the sewershed. This uncertainty represents opportunities for future work.

Source diversity was evident in results from Buncombe, Greenville, and Roanoke Rapids, which likely reflected both surface and subsurface processes during wet conditions. In some systems, surface inflows may enter through gutters, manholes, or illegal connections. Rising groundwater levels and saturated soils enhance infiltration through defective infrastructure. In Northern Sweden, Panasiuk et al., 2022) observed higher dilution and declining ammonium concentrations during rain events, suggesting new inflow pathways became active during wet weather. Similarly, rainfall events in Ningbo City, China, led to increased flows in both separate and combined sewer systems, linked to both surface inflow and groundwater infiltration (Wang et al., 2024).

Some facilities displayed consistently high source diversity despite rainfall conditions. Wilson and Jacksonville, for example, showed three or more sources even during dry periods, suggesting that chronic I&I problems extend beyond storm-driven inputs. This may be explained by a combination of factors, including infrastructure deterioration, direct influence from shallow groundwater tables, and perhaps the number of direct stormwater connections. In such cases, these sewer systems appear to operate under a baseline of multiple I&I sources.

In contrast, facilities such as Mallard Creek and McDowell Creek showed little or no effect of rainfall on source diversity. These systems rarely had more than one contributing source across all precipitation categories, consistent with their low dilution values and limited evidence of I&I impacts. The stability of these sites suggests well-maintained infrastructure and favorable geophysical conditions (deeper water tables or steeper topography) reduced the likelihood of infiltration. These contrasting patterns suggest that antecedent rainfall (location, intensity) can strongly influence I&I source diversity in some systems; others are more affected by structural issues and are resilient to weather variability.

Increased source diversity adds complexity, as multiple mechanisms must be addressed to reduce I&I effectively. Understanding when and how different pathways are activated is key to developing targeted interventions. Variability in precipitation patterns, groundwater levels, and the condition and management of sewer infrastructure also influence the extent and dynamics of I&I (Sebo & McDonald, 2022). This study did not determine the relative importance of these factors, but the results highlight that both environmental setting and infrastructure management need to be considered when interpreting I&I dynamics.

5. Conclusions

This study assessed inflow and infiltration dynamics across diverse wastewater treatment plants using organic matter fluorescence, modeling, flow rate, and precipitation data. The findings demonstrate that I&I patterns are highly variable across facilities and are shaped by a combination of factors, including hydrogeological setting, sewer infrastructure condition, and rainfall variability.

The application of the FluorMod model was validated under controlled laboratory conditions, confirming its ability to accurately identify and quantify I&I sources, even at high levels of dilution, when source signals remain above the 5% detection threshold. These validation experiments support applying FluorMod in various field conditions as a promising forensic tool for sewer repair and maintenance and to investigate effects of climate change on flooding of municipal infrastructure by extreme rainfall and sea level rise.

Across the WWTPs analyzed, influent dilution patterns revealed three general categories of I&I behavior: (1) chronic infiltration systems dominated by persistent groundwater inputs (e.g., Wilson and Jacksonville), (2) mixed-source systems exhibiting variable contributions from both groundwater and rainwater depending on antecedent conditions (e.g., Greenville and Roanoke Rapids), and (3) rainfall-responsive systems with minimal dry-weather I&I and occasional, inconsistent, dilution following precipitation events (e.g., Buncombe, Marion, McDowell Creek). These classifications were supported by time series analysis, correlations with antecedent precipitation, and modeled I&I source contributions.

Waste water treatment plants in the Coastal Plain generally experienced higher groundwater contributions and persistent dilution. This likely resulted from sewer lines situated in shallow water tables and saturated soils, facilitating chronic infiltration. In contrast, facilities in the Piedmont region tended to exhibit limited baseline I&I. Intermediate behaviors were observed at several facilities, where potential factors, such as damaged infrastructure or geophysical conditions, may permit both episodic inflow and sustained groundwater entry.

Antecedent precipitation (AP_5) influenced the magnitude of dilution and the diversity of contributing I&I sources. At several facilities, increased AP_5 was associated with a higher number of sources, indicating that storm events activate multiple inflow and infiltration pathways. However, this relationship varied across systems: some facilities exhibited consistently high source diversity regardless of rainfall, while others showed little change. This variation highlights the complexity of I&I responses and suggests that both environmental drivers and infrastructure characteristics modulate system behavior.

6. Recommendations

Climate change is expected to increase the frequency and intensity of extreme precipitation, amplifying I&I vulnerabilities. Therefore, tools such as FluorMod, which support ongoing monitoring and enhanced diagnostic capabilities, are essential. Broader implementation of this approach, incorporating additional analysis such as geospatial data with sewer infrastructure, soil type, groundwater dynamics, and other factors, will be critical for advancing both scientific understanding and practical mitigation of I&I impacts in wastewater systems.

FluorMod offers WWTP operators a valuable tool for estimating I&I extent and variability. As part of this study, individualized reports were developed for each participating WWTP, summarizing the methodology and presenting results relevant to addressing I&I challenges. Meetings were held with key stakeholders, including representatives from the Roanoke Rapids Sanitary District and Charlotte Water, the primary agencies responsible for wastewater collection and treatment in Roanoke Rapids and Charlotte, respectively. The findings aligned closely with the utility's existing knowledge of its systems, reinforcing the credibility of the fluorescence-based approach. Both entities recognized the potential of FluorMod as a complementary tool for identifying high I&I zones when used alongside established field techniques such as CCTV inspection and in-situ flow monitoring.

FluorMod's utility extends beyond I&I monitoring. The model can also be adapted to detect exfiltration, or the leakage of wastewater out of sewer systems into surrounding environments. By sampling surface or groundwater near suspected damaged sewer areas and analyzing fluorescence signals, FluorMod can estimate wastewater leakage. One of the key innovations of this tool is its customizability: users can include or exclude specific sources within the model based on their research objectives, enhancing flexibility and precision.

A final innovation of this project is the model's adaptability to multiple programming languages and its potential for integration into web-based platforms, making the tool more accessible and user-friendly for a broad range of practitioners. FluorMod is publicly available as Google Colaboratory script in Python. R code is available from the authors[1]. This flexibility supports wider adoption in both academic and operational contexts.

[1] Following publication of a manuscript from this work that is in preparation, the full dataset will be made publicly available through the NC State Dryad Data Repository.

References

Englande, A., Krenkel, P., & Shamas, J. (2015). Wastewater Treatment &Water Reclamation. *Reference Module in Earth Systems and Environmental Sciences*, B978-0-12-409548-9.09508-7. https://doi.org/10.1016/B978-0-12-409548-9.09508-7

Bryan, J. G., Hoff, P. D., & Osburn, C. L. (2025). Linear Source Apportionment Using Generalized Least Squares. *Technometrics*, *67*(1), 1–16. https://doi.org/10.1080/00401706.2024.2379850

Bryan, J., Hoff, P., & Osburn, C. L. (2023). Routine estimation of dissolved organic matter sources using fluorescence data and linear least squares. *Environmental Science and Technology: Water*, *submitted*.

Budd, E., Babcock, R. W., Spirandelli, D., Shen, S., & Fung, A. (2020). Sensitivity Analysis of a Groundwater Infiltration Model and Sea-Level Rise Applications for Coastal Sewers. *Water 2020, Vol. 12, Page 923*, *12*(3), 923. https://doi.org/10.3390/W12030923

Cahoon, L. B., & Hanke, M. H. (2017). Rainfall effects on inflow and infiltration in wastewater treatment systems in a coastal plain region. *Water Science and Technology*, *75*(8), 1909–1921. https://doi.org/10.2166/WST.2017.072

Carey, R. O., & Migliaccio, K. W. (2009). Contribution of wastewater treatment plant effluents to nutrient dynamics in aquatic systems. *Environmental Management*, *44*(2), 205–217. https://doi.org/10.1007/S00267-009-9309-5/FIGURES/4

Choi, N., & Schmidt, A. (2020). Identifying sources of rainfall derived infiltration and inflow using impulse response functions. *Authorea Preprints*. https://doi.org/10.22541/AU.158679896.68487959

Coble, P. G. (2007). Marine optical biogeochemistry: The chemistry of ocean color. *Chemical Reviews*, *107*(2), 402–418. https://doi.org/10.1021/cr050350

Dirckx, G., Van Daele, S., & Hellinck, N. (2016). Groundwater Infiltration Potential (GWIP) as an aid to determining the cause of dilution of waste water. *Journal of Hydrology*, *542*, 474–486. https://doi.org/10.1016/J.JHYDROL.2016.09.020

Durso, F., Solomon, J. D., & Colson, K. (2019). North Carolina's Bold Water and Wastewater Infrastructure Plan. *Journal AWWA*, *111*, 38–43. https://www.jstor.org/stable/26653948?seq=1

Eskaf, S., & Vulpis, R. (2021). *Estimating The Statewide Water And Wastewater Capital Spending Plans Of North Carolina's Local Governments*. https://efc.sog.unc.edu/resource/estimating-the-statewide-water-and-wastewater-capital-spending-plans-of-north-carolinas-local-governments/

FENNER, R. A. (1990). Excluding Groundwater Infiltration into New Sewers. *Water and Environment Journal*, *4*(6), 544–551. https://doi.org/10.1111/J.1747-6593.1990.TB01468.X

Flood, J. F., & Cahoon, L. B. (2011). Risks to Coastal Wastewater Collection Systems from Sea-Level Rise and Climate Change. *Journal of Coastal Research*, *274*(4), 652–660. https://doi.org/10.2112/JCOASTRES-D-10-00129.1

Hagen, A. B., Cangialosi, J. P., Chenard, M., Alaka, L., & Delgado, S. (2025). National Hurricane Center Tropical Storm Report, Hurricane Helene (AL092024). In *Monthly Weather Review* (Vol. 145, Issue 5). American Meteorological Society. https://www.nhc.noaa.gov/data/tcr/AL092024_Helene.pdf

Hanke, S. H., & Wentworth, R. W. (1981). On the Marginal Cost of Wastewater Services. *Land Economics*, *57*(4), 558. https://doi.org/10.2307/3145671

Hoff, P., & Osburn, C. L. (2025). Evaluation of the linear mixing model in fluorescence spectroscopy. *Next Research*, *2*(3), 100540. https://doi.org/10.1016/J.NEXRES.2025.100540

Karpf, C., & Krebs, P. (2011). Quantification of groundwater infiltration and surface water inflows in urban sewer networks based on a multiple model approach. *Water Research*, *45*(10), 3129–3136. https://doi.org/10.1016/J.WATRES.2011.03.022

Kothawala, D. N., Murphy, K. R., Stedmon, C. A., Weyhenmeyer, G. A., & Tranvik, L. J. (2013). Inner filter correction of dissolved organic matter fluorescence. *Limnology and Oceanography: Methods*, *11*(12), 616–630. https://doi.org/10.4319/LOM.2013.11.616

Kracht, O., Gresch, M., & Gujer, W. (2007). A stable isotope approach for the quantification of sewer infiltration. *Environmental Science and Technology*, *41*(16), 5839–5845. https://doi.org/10.1021/ES062960C/SUPPL_FILE/ES062960CSI20070705_091436.PDF

Osburn, C. L., Handsel, L. T., Peierls, B. L., & Paerl, H. W. (2016). Predicting Sources of Dissolved Organic Nitrogen to an Estuary from an Agro-Urban Coastal Watershed. *Environmental Science and Technology*, *50*(16), 8473–8484. https://doi.org/10.1021/acs.est.6b00053

Panasiuk, O., Hedström, A., Langeveld, J., & Viklander, M. (2022). Identifying sources of infiltration and inflow in sanitary sewers in a northern community: comparative assessment of selected methods. *Water Science and Technology*, *86*(1), 1–16. https://doi.org/10.2166/WST.2022.151

Reinhart, B. J., Reinhart, A., & Alaka, L. (2025). *National Hurricane Center Tropical Cyclone Report, Hurricane Debby (AL042024)*. https://www.google.com/url?sa=t&source=web&rct=j&opi=89978449&url=https://www.nhc.noaa.gov/data/tcr/AL042024_Debby.pdf&ved=2ahUKEwi-2pqFuPyQAxVxF1kFHUGUA6cQFnoECCMQAQ&usg=AOvVaw2Mj4LBCpukfXOJx1_HWMLD

Roghani, B., Rokstad, M. M., & Tscheikner-Gratl, F. (2024). Quantifying Excessive Water Inflow in Urban Sewer Systems: A Case Study in a mid-sized Norwegian municipality. *Vann*, 307–314. https://www.researchgate.net/publication/387784597_Quantifying_Excessive_Water_Inflow_in_Urban_Sewer_Systems_A_Case_Study_in_a_mid-sized_Norwegian_municipality

Rossi, R. J., & Toran, L. (2019). Exploring the potential for groundwater inundation in coastal US cities due to interactions between sewer infrastructure and global change. *Environmental Earth Sciences*, *78*(8), 258-. https://doi.org/10.1007/S12665-019-8261-9/FIGURES/5

Saletti, A. O. (2021). *Infiltration and inflow to wastewater sewer systems - A literature review on risk management and decision support*. Chalmers University of Technology. https://research.chalmers.se/en/publication/522159

Sebo, S., & McDonald, W. (2022). Influence of Sewershed Characteristics on Rainfall-Derived Inflow and Infiltration. *JAWRA Journal of the American Water Resources Association*, *58*(6), 1483–1496. https://doi.org/10.1111/1752-1688.13051

Sowby, R. B., & Jones, D. R. (2022). A Practical Statistical Method to Differentiate Inflow and Infiltration in Sanitary Sewer Systems. *Journal of Environmental Engineering*, *148*(1), 06021006. https://doi.org/10.1061/(ASCE)EE.1943-7870.0001962/ASSET/5D00DDE6-F62A-4894-9F3A-99B9D4972B06/ASSETS/IMAGES/LARGE/FIGURE3.JPG

Staufer, P., Scheidegger, A., & Rieckermann, J. (2012). Assessing the performance of sewer rehabilitation on the reduction of infiltration and inflow. *Water Research*, *46*(16), 5185–5196. https://doi.org/10.1016/J.WATRES.2012.07.001

US Environmental Protection Agency. (2004). *Primer for Municipal Wastewater Treatment Systems*. https://www.epa.gov/sites/default/files/2015-09/documents/primer.pdf

von Storch, H., & Swiers, F. W. (1999). *Statistical Analysis in Climate Research*. Cambridge University Press. https://www.google.com/books/edition/Statistical_Analysis_in_Climate_Research/bs8hAwAAQBAJ?hl=en&gbpv=1&dq=Statistical+analysis+in+climate+research&pg=PT11&printsec=frontcover

Wang, Y., Huang, B., & Zhu, D. Z. (2024). Assessment of rainfall-derived inflow and infiltration in sewer systems with machine learning approaches. *Water Science and Technology*, *89*(8), 1928–1945. https://doi.org/10.2166/WST.2024.115

Wittenberg, H., & Aksoy, H. (2010). Groundwater intrusion into leaky sewer systems. *Water Science and Technology*, *62*(1), 92–98. https://doi.org/10.2166/WST.2010.287

Wride, D., Chen, M., & Johnstone, R. (2004). Characterizing the Spatial Variability of Rainfall Across a Large Metropolitan Area. *Proceedings of the 2004 World Water and Environmetal Resources Congress: Critical Transitions in Water and Environmetal Resources Management*, 1–10. https://doi.org/10.1061/40737(2004)155

Wright, L. T., Dent, S., Mosley, C., Kadota, P., & Djebbar, Y. (2001). Comparing Rainfall Dependent Inflow and Infiltration Simulation Methods. *Journal of Water Management Modeling*. https://doi.org/10.14796/JWMM.R207-16

Zeydalinejad, N., Javadi, A. A., & Webber, J. L. (2024). Global perspectives on groundwater infiltration to sewer networks: A threat to urban sustainability. *Water Research*, *262*, 122098. https://doi.org/10.1016/J.WATRES.2024.122098

Zhang, K., & Parolari, A. J. (2022). Impact of stormwater infiltration on rainfall-derived inflow and infiltration: A physically based surface–subsurface urban hydrologic model. *Journal of Hydrology*, *610*, 127938. https://doi.org/10.1016/j.jhydrol.2022.127938

Appendix 1.

List of abbreviations and symbols.

Abbreviations

AP_5 = 5-day antecedent precipitation

CCTV = closed-circuit television

CSO = combined sewer overflow

DHHS = Department of Health and Human Services

DOM = dissolved organic matter

EEM = excitation-emission matrix

Em = emission

Ex = excitation

GF/F = glass fiber filter

HDPE = high density polyethylene

IQR = interquartile range

I&I = inflow and infiltration

LOD = limit of detection

MGD = million gallons per day

NCSU = North Carolina State University

NNLS = non-negative least squares

PARAFAC = parallel factor analysis

PVC = polyvinyl chloride

Q1 = 25th percentile

Q3 = 75th percentile

QSU (or QSE) = quinine sulfate unit (or equivalent)

RSS = residual sum of squares

RTS = Regress-Then-Sum

TSS = total sum of squares

WWTP = wastewater treatment plant

<u>Symbols</u>

α = absorption coefficient (m^{-1})

A = absorbance (unitless)

λ = wavelength (nm)

L = pathlength (m)

MΩ = megaohm

m = meter

nm = nanometer

p = p-value

ppb = part per billion

r = Pearson correlation coefficient

R^2 = coefficient of determination

X^2 = chi-square

Appendix 2.

<u>List of presentations, publications, and thesis (* = student author)</u>

Osburn, C. L. (2024). Determining the dilution of wastewater treatment plant influent by inflow and infiltration using organic matter fluorescence. Water Resources Research Institute 26th Annual Conference, Raleigh, NC 20-21 March 2024.

Cornejo, S. G.*, Osburn, C. L. (2024). Improved Quantification of Stormwater Dilution in Wastewater Treatment Plant Influent Using Organic Matter Fluorescence. North Carolina Coastal Conference, New Bern, NC, 13-14 November 2024

Osburn, C. L. (2025). Quantification of Stormwater Dilution in Wastewater Treatment Plant Influent Using Organic Matter Fluorescence. Water Resources Research Institute 27th Annual Conference, Raleigh, NC 19—20 March 2025.

Cornejo, S. G.*, Osburn, C. L. (2025). Improved quantification of stormwater dilution of wastewater treatment plant influent using organic matter fluorescence. ASLO Aquatic Sciences Meeting, Charlotte, NC, 29 March 2025.

Hoff, P., & Osburn, C. (2025). Evaluation of the linear mixing model in fluorescence spectroscopy. Next Research, 100540.

Cornejo Zepeda, S. G.* (2025). Improved Quantification of Dilution in Wastewater Treatment Plant Influent using Organic Matter Fluorescence. Master's Thesis. North Carolina State University. Raleigh, NC. 88 pp.

<u>Technology Transfer & Communication of Results</u>

Cornejo, S. G. & Osburn, C. L. (2025) INFLOW AND INFILTRATION RESULTS REPORT. – These reports were sent to each participating WWTP or sewer authority for the following municipalities: Buncombe, Charlotte (including the WWTPs: Sugar Creek, McDowell Creek, Mallard Creek and Irwin Creek), Greenville, Marion, Roanoke Rapids and Wilson.

Virtual meetings were held to discuss results contained in the reports, explain the technology, advise on implementation of the methods, and to explore future collaborations. District or authority and date of meeting are noted below.

March 28, 2024 - Groundwater sampling project for fluorescence analysis, Wake County
May 1, 2024 - In-person meeting at Wake County Water Quality Lab
February 5, 2025 - Groundwater Fluorescence Results, Wake County
June 23, 2025·- Orange Water And Sewer Authority (OWASA) Meeting
August 27, 2025 - Presentation of Results Roanoke Rapids

- Pilot project initiated November 2025

September 4, 2025 - Presentation of Results Charlotte Water

Supporting Information

Figure S1. Correlation between 5-day antecedent precipitation and influent flow rates. (A) Buncombe (B), Irwin Creek (C), Jacksonville (D), Mallard Creek (E), Marion (F), Roanoke Rapids, and Sugar Creek WWTPs (G).

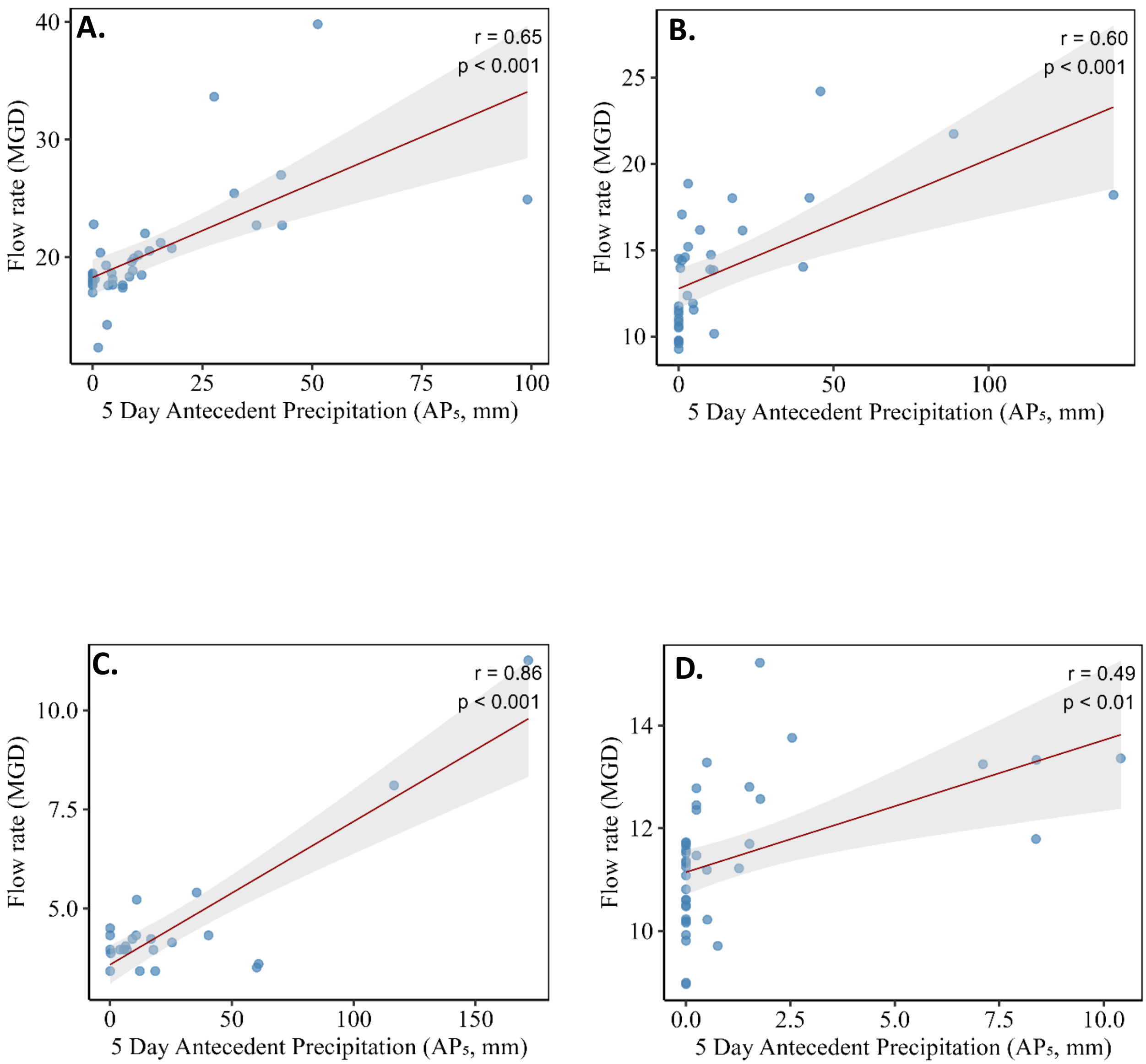

Figure S1. Continued.

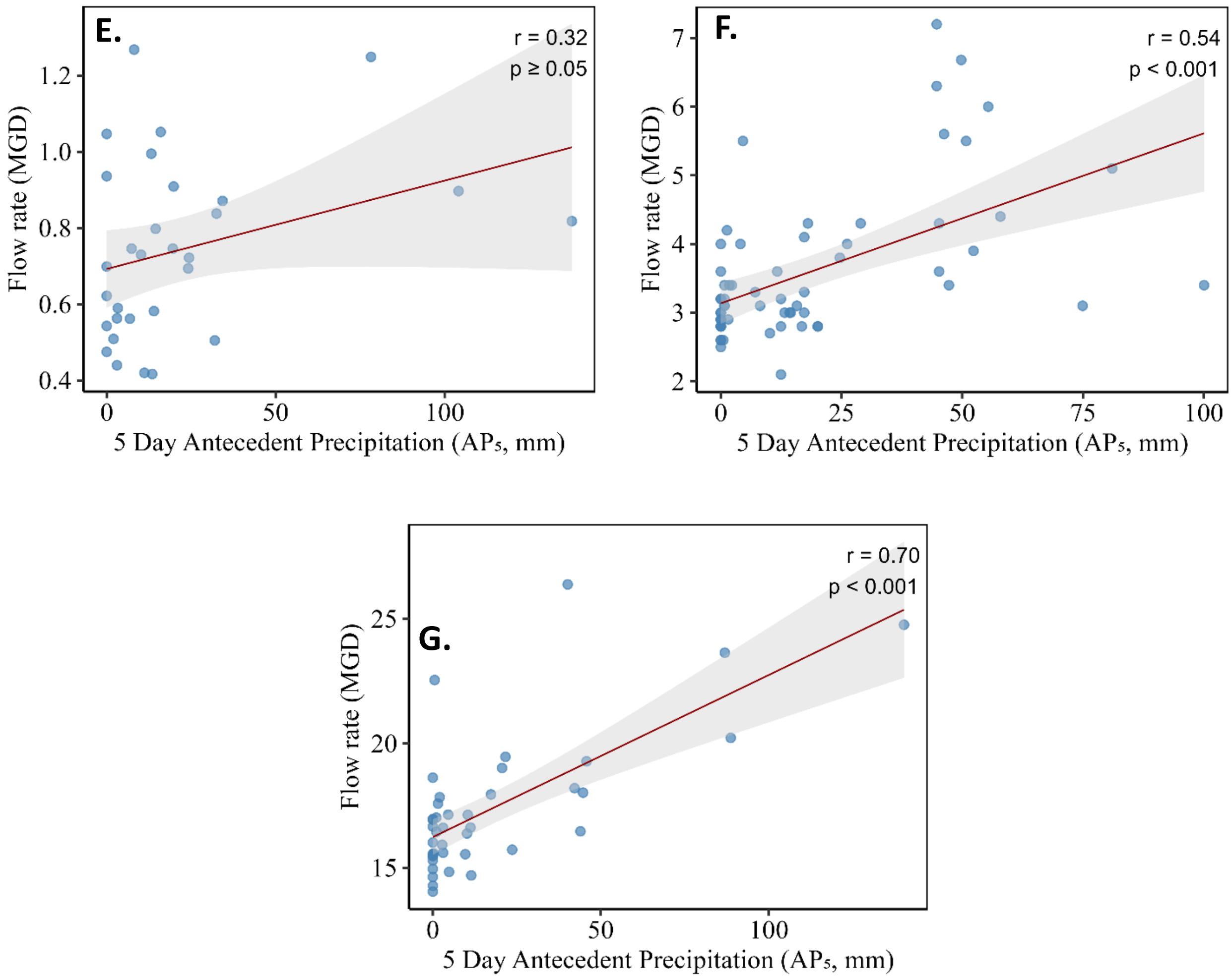

Figure S2. Influent flow, precipitation, and source contributions at Greenville WWTP. (Top) Influent flow rates (million gallons per day, MGD) and antecedent 5-day cumulative precipitation (mm). (Bottom) Relative contributions (%) of wastewater and other water sources to influent dilution over time.

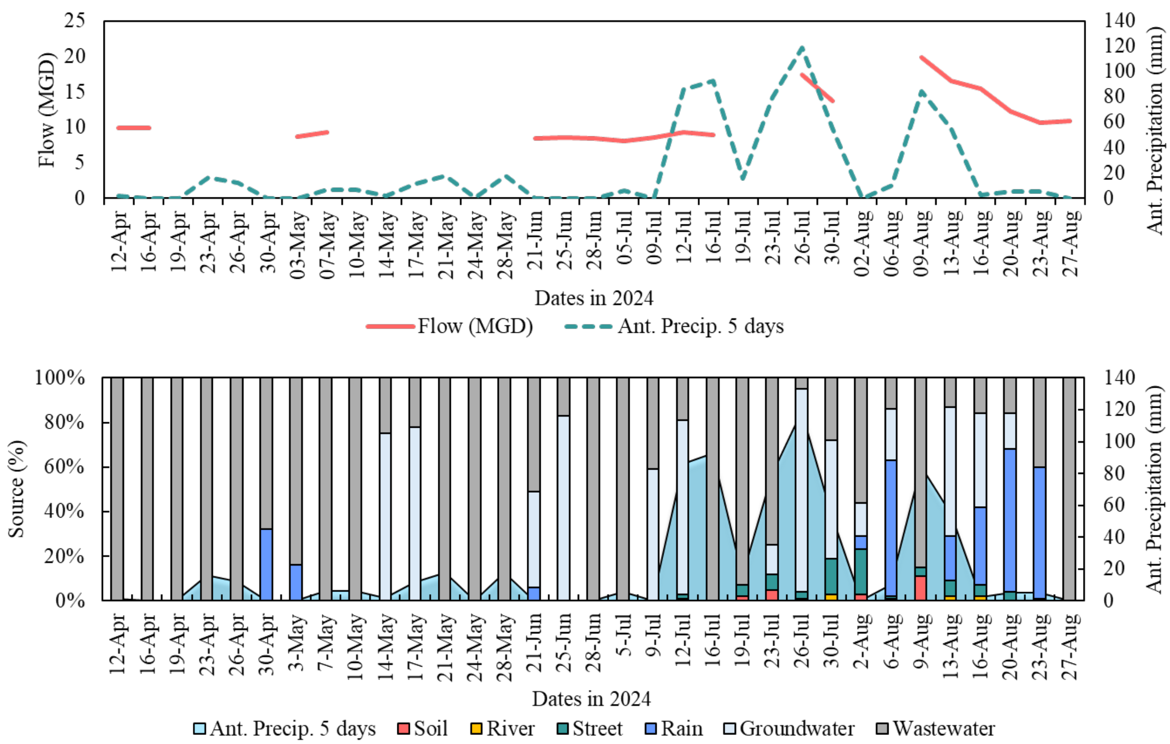

Figure S3. Influent flow, precipitation, and source contributions at Jacksonville WWTP. (Top) Influent flow rates (million gallons per day, MGD) and antecedent 5-day cumulative precipitation (mm). (Bottom) Relative contributions (%) of wastewater and other water sources to influent dilution over time.

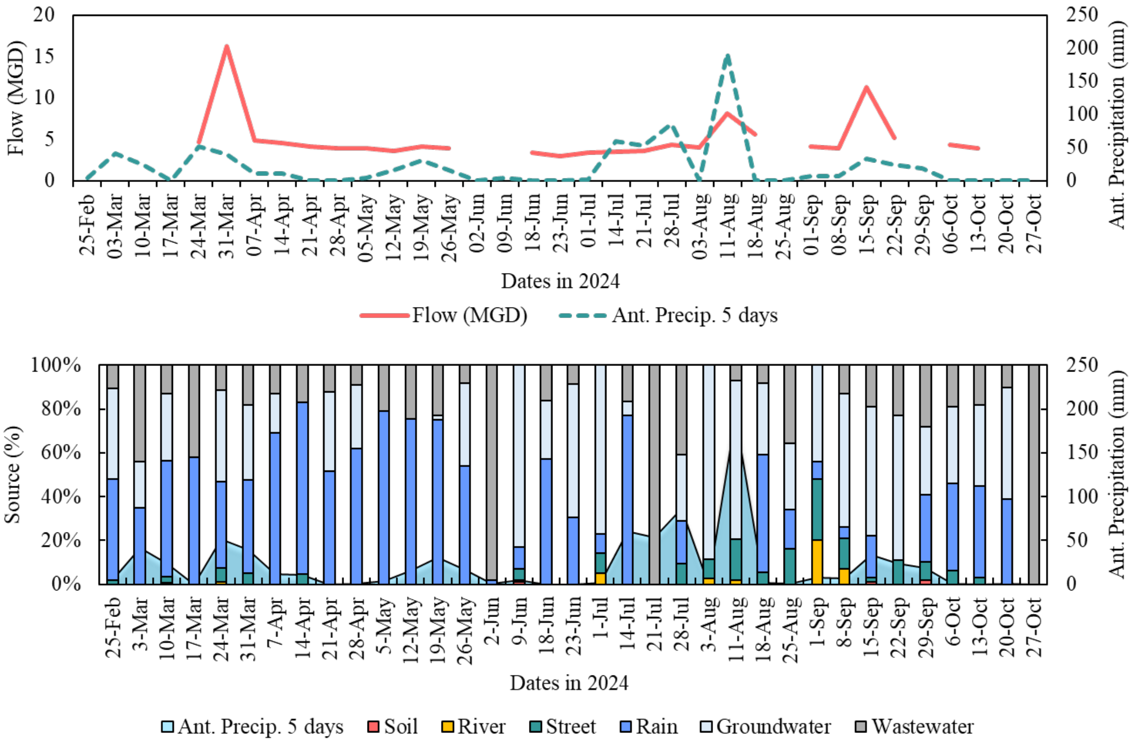

Figure S4. Influent flow, precipitation, and source contributions at Mallard WWTP. (Top) Influent flow rates (million gallons per day, MGD) and antecedent 5-day cumulative precipitation (mm). (Bottom) Relative contributions (%) of wastewater and other water sources to influent dilution over time.

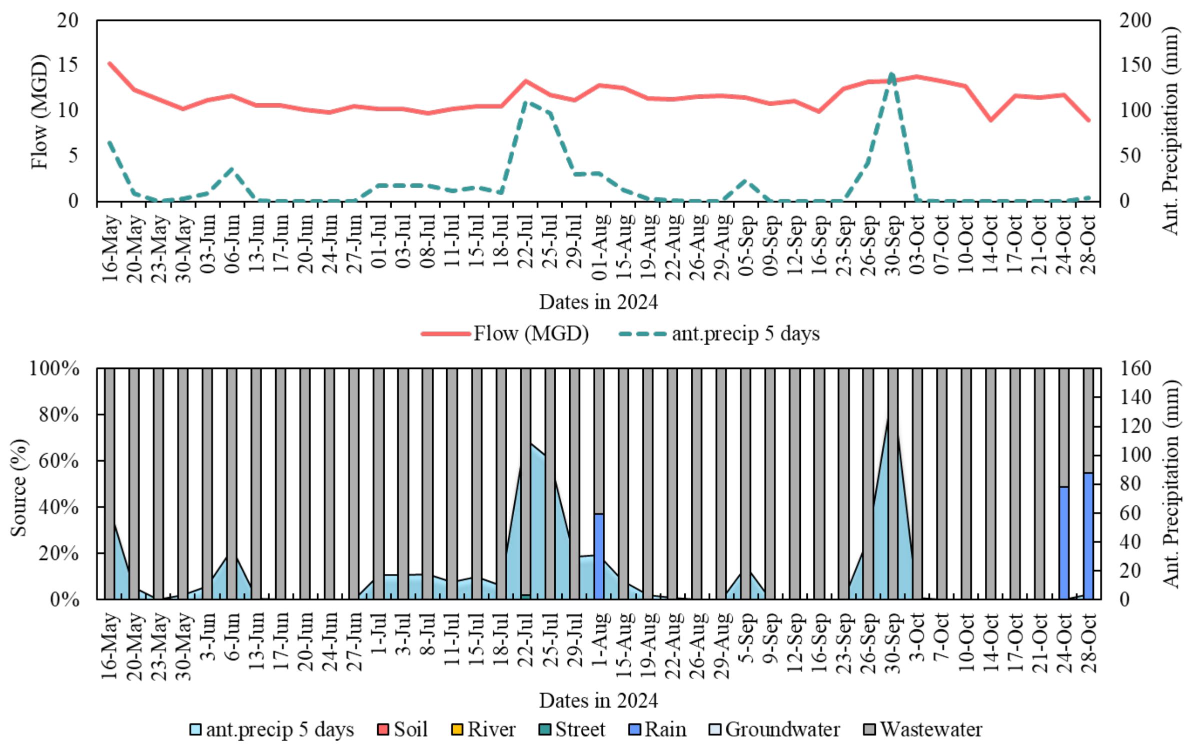

Figure S5. Influent flow, precipitation, and source contributions at Marion WWTP. (Top) Influent flow rates (million gallons per day, MGD) and antecedent 5-day cumulative precipitation (mm). (Bottom) Relative contributions (%) of wastewater and other water sources to influent dilution over time.

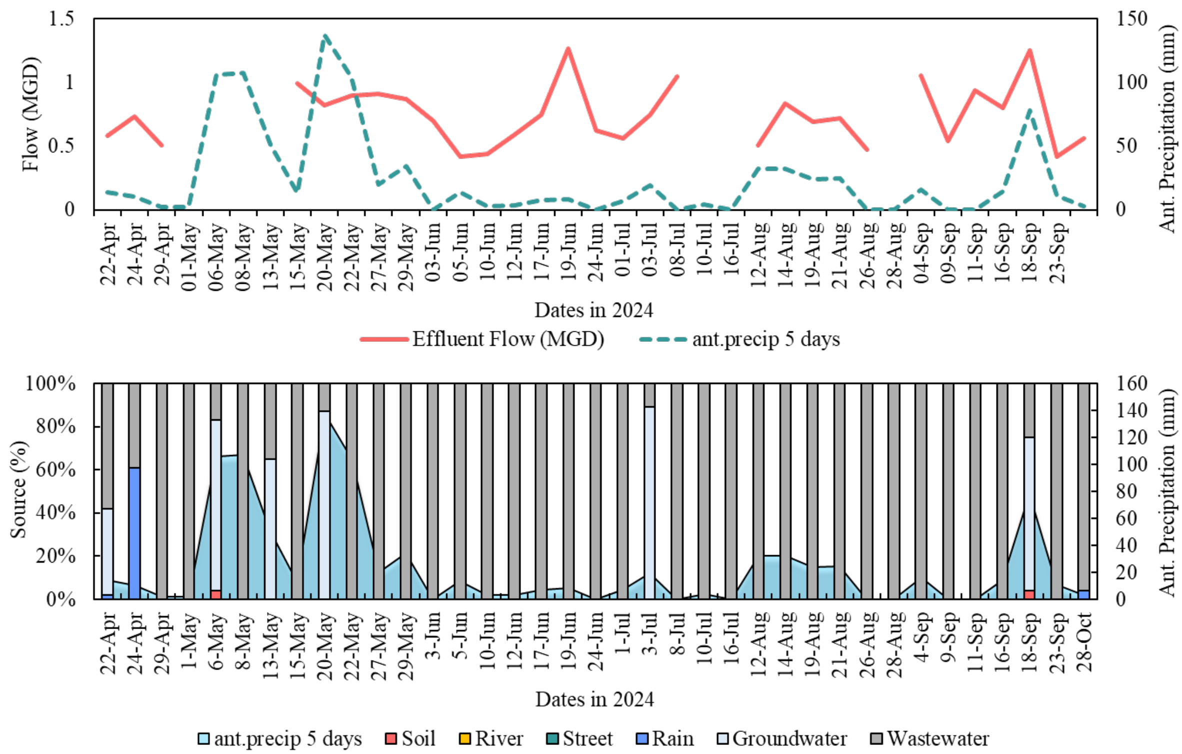

Figure S6. Influent flow, precipitation, and source contributions at McDowell WWTP. (Top) Influent flow rates (million gallons per day, MGD) and antecedent 5-day cumulative precipitation (mm). (Bottom) Relative contributions (%) of wastewater and other water sources to influent dilution over time.

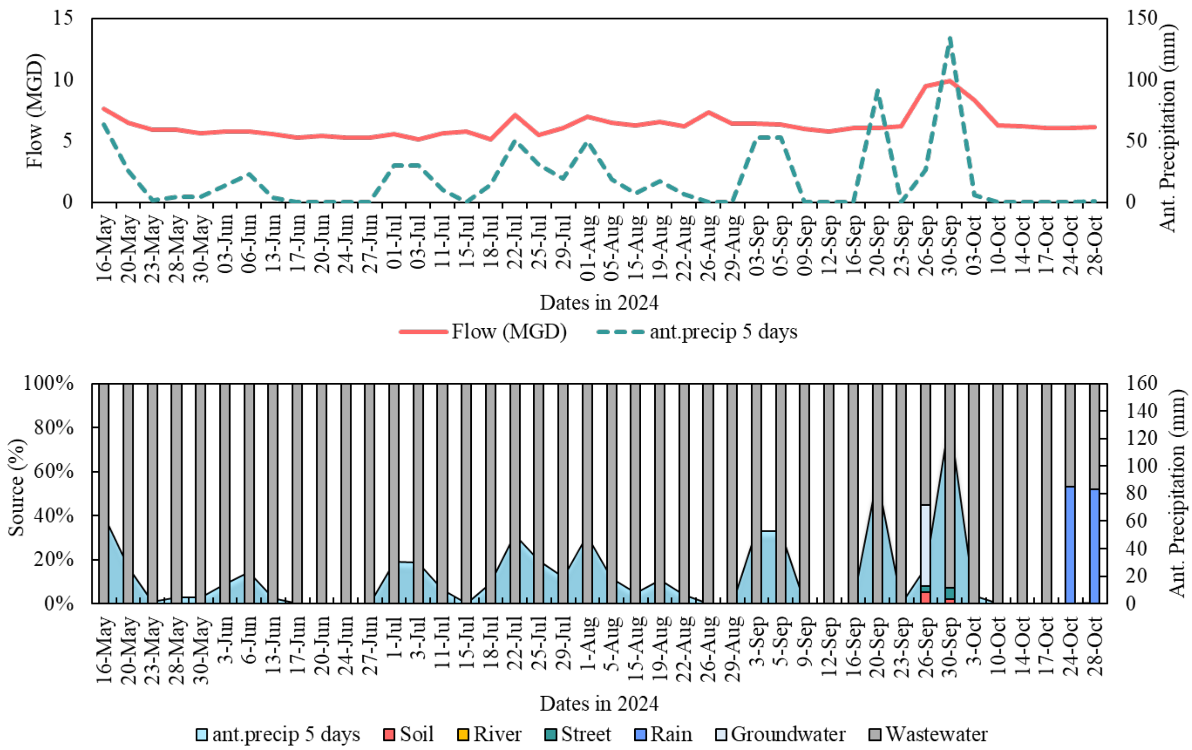

Figure S7. Influent flow, precipitation, and source contributions at Roanoke Rapids WWTP. (Top) Influent flow rates (million gallons per day, MGD) and antecedent 5-day cumulative precipitation (mm). (Bottom) Relative contributions (%) of wastewater and other water sources to influent dilution over time.

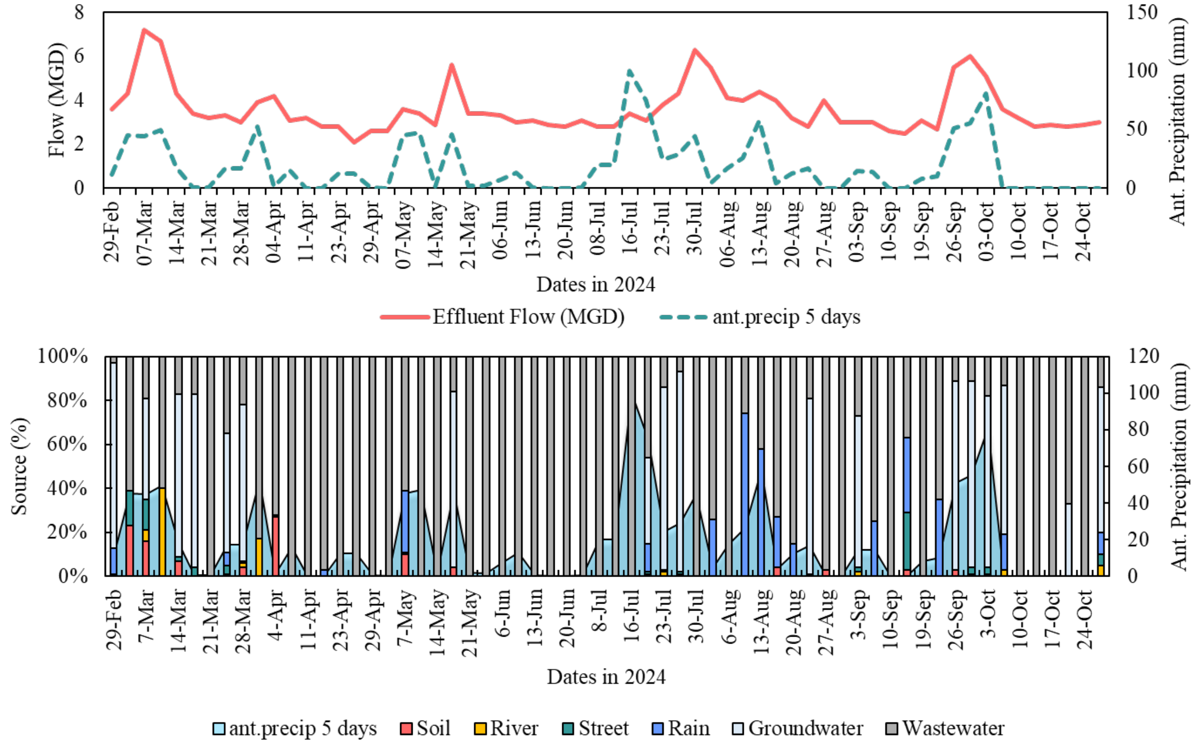

Figure S8. Influent flow, precipitation, and source contributions at Sugar Creek WWTP. (Top) Influent flow rates (million gallons per day, MGD) and antecedent 5-day cumulative precipitation (mm). (Bottom) Relative contributions (%) of wastewater and other water sources to influent dilution over time.